國 立 交 通 大 學

電子工程學系 電子研究所碩士班

碩 士 論 文

移動 **WiMAX** 系統之導引碼輔助

疊代式通道估測

Pilot-Assisted Iterative Channel Estimation for

Mobile WiMAX Systems
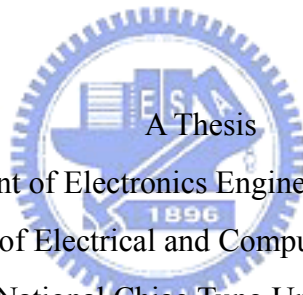
研 究 生：陳錫祺

指導教授：簡鳳村 博士

中 華 民 國 九 十 六 年 七 月

移動 WiMAX 系統之導引碼輔助疊代式通道估測

Pilot-Assisted Iterative Channel Estimation for Mobile WiMAX Systems

研究生: 陳錫祺

指導教授: 簡鳳村

Student: Shi-Chi Chen

Advisor: Dr. Feng-Tsun Chien

國 立 交 通 大 學

電 子 工 程 學 系　電 子 研 究 所 碩 士 班

碩 士 論 文

A Thesis

Submitted to Department of Electronics Engineering & Institute of Electronics

College of Electrical and Computer Engineering

National Chiao Tung University

in Partial Fulfillment of the Requirements

for the Degree of Master

in

Electronics Engineering

June 2007

HsinChu, Taiwan, Republic of China

中華民國九十六年七月

移動 WiMAX 系統之導引碼輔助

疊代式通道估測

研究生: 陳錫祺　　　　　　　　　　　　指導教授: 簡鳳村 博士

國立交通大學

電子工程學系 電子研究所碩士班

摘要

正交分頻多工系統為新一代無線通訊系統最常使用的技術,如 IEEE 802.11 a/g/n, IEEE 802.16, IEEE 802.20,數位電視,數位廣播等許多系統均採用此技術。移動傳輸是未來無線通訊系統的趨勢之一,如 IEEE 802.16-2005 可支援到車速 120 km/hr,而 IEEE 802.20 更可以支援到車速 250 km/hr。許多通道估測法,使用大量的導引符號,以及緩衝暫存器來估測通道。在本論文中,我們使用兩種通道估測,decision directed 和 expectation maximization。此通道估測可追蹤時變通道,以及使用少量導引符號。最後,藉由電腦模擬驗證此一新演算法在移動的環境中並使用 IEEE 802.16-2005 的規格下,可有效的改善錯誤率。

Pilot-Assisted Iterative Channel Estimation for Mobile WiMAX Systems

Student: Shi-Chi Chen   Advisor: Dr. Feng-Tsun Chien

Department of Electronic Engineering &
Institute of Electronics
National Chiao Tung University

Abstract

Orthogonal Frequency Division Multiplexing (OFDM) is a popular technique in modern wireless communications. There are many systems adopting the OFDM technique, such as IEEE 802.11 a/g/n, IEEE 802.16, IEEE 802.20, and Digital Video Broadcasting, etc. On the other hand, mobility is an important issue that needs to be taken into account in the design of future wireless communication systems. For example, IEEE 802.16-2005 supports vehicle speed up to 120 km/hr, and IEEE 802.20 supports vehicle speed up to 250 km/hr, causing the channel seen by the receiver time-varying. Some channel estimators use a large number of pilot symbols to estimate the channel parameters, or use buffer to obtain desired channel parameters. In this thesis, we show two channel estimation approaches, namely the decision directed based and expectation maximization based approaches that can track the time-varying channel vectors with less insertion of pilot symbols. Finally, we evaluate the performance of the proposed systems under mobility using IEEE 802.16-2005 standard and confirm that it achieves good SER performance.

誌謝

　　這篇論文能夠順利完成，最重要感謝的人是我的指導教授 簡鳳村 老師。在這二年的研究生涯中，老師不僅在做研究上給予指導，讓我在知識的探索上獲益良多，同時也關心我們的日常生活。

　　另外，要感謝的是與我在通訊領域之中一起討論、研究的洪崑健與林鴻志學長，謝謝你們熱心地幫我解決了許多通訊方面相關的疑問。也感謝從大學到研究所都一直共同打拼的耀鈞、柏昇、政達、介遠、志岡、凱庭、依翎，在修課中遇到問題時，大家互相討論，解決難題，讓我在這之中成長許多。也感謝實驗室的其他成員，在碩士這兩年中帶給我歡樂、成長，在生活上給我支持、勉勵，使我充滿信心。也感謝通訊電子與訊號處理實驗室(commlab)，提供了充足的軟硬體資源，讓我在研究中不虞匱乏。

　　在此僅以這篇論文獻給所有幫助過我，陪伴我走過這一段歲月的師長，同學，朋友與家人，謝謝！

誌於 2007.7 風城交大

錫祺

iii

Contents

List of Figures

List of Tables

Chapter 1
Introduction

1.1 Significance

Wireless communication systems have been in use for quite a long time. Many standards are available based on which user devices communicate, but the present standards fail to provide sufficient data rate, when the user is moving at high speed. Broadband wireless access is an appealing way to provide flexible and easily-to-deploy solution for high speed communications. In view of this requirement for future mobile wireless communication systems, the 802.16 standard has been proposed by Institute of Electrical and Electronic Engineers (IEEE) [1][3]

The WiMAX (Worldwide Interoperability for Microwave Access) Forum is committed to providing optimized solutions for fixed, nomadic, portable and mobile broad band wireless access. Two versions of WiMAX address the demand for different type of access:

- **IEEE 802.16-2004:** This is based on the 802.16-2004 version of the IEEE 802.16 standard. It uses Orthogonal Frequency Division Multiplexing (OFDM) and supports fixed and nomadic access in Line of Sight (LOS) and Non Line of Sight (NLOS) environments. For LOS environment, the frequency range in 802.16d is from $2\,GHz$ to $66\,GHz$ and Single Carrier (SC) is mainly adopted as the

transmission scheme. For NLOS environment, it focuses on the Broadband Wireless Access (BWA), where the frequency band ranges from $2\,GHz$ to $10\,GHz$. In physical layer (PHY), NLOS temps to adopt OFDM and OFDMA techniques.

- **IEEE 802.16-2005:** optimized for dynamic mobile radio channels. This version is based on the IEEE 802.16-2005 amendment and provides support for handoffs and roaming. The choice of the subcarrier number becomes more flexible since it provides four options, 128, 512, 1024, 2048, in contrast to the single choice of 2048 in IEEE 802.16-2004. the frequency band ranges from $2\,GHz$ to $6\,GHz$.

Orthogonal Frequency Division Multiplexing (OFDM) is a popular technique in modern wireless communication systems. In an OFDM system, the bandwidth is divided into several orthogonal subchannels for transmission. A cyclic prefix (CP) is inserted before each symbol. Therefore, if the delay spread of the channel is shorter than the length of the cyclic prefix, the intercarrier symbol interference (ISI) can be eliminated due to the cyclic prefix. On the other hand, subcarriers in OFDM system are orthogonal to each other over time-invariant channels, so the conventional OFDM system only requires one-tap equalizers [5] to compensate the channel response. This characteristic simplifies the design of the OFDM receiver, and for this reason, the OFDM technique is widely used in wireless communication systems.

1.2 Motivation

Mobile transmission is a trend in future wireless communications. Many systems support the mobile transmission. While the OFDM system is applied in mobile environments, the

reliability of OFDM is limited because of the time-varying nature of the channel. A simple

solution of the channel estimation is Pilot-Symbol-Aided. This solution makes each symbol

has its own pilot. For these pilots, we can estimate these channels respective. Obviously, this

way decreases data rate of transmission. We want to reduce pilot number of OFDM system.

We assumed that the power spectral density of channel environment is modeled using

Jakes' U-shaped function corresponding to the uniform angular distribution of the received

energy at the receiver antenna [27]. In the case, the covariance function of the channel process

is given by

$$C_h\left(m\right) = E\left\{h_k, h^*_{k-m}\right\} = \sigma_h^2 J_0\left(\Omega_d m\right)$$
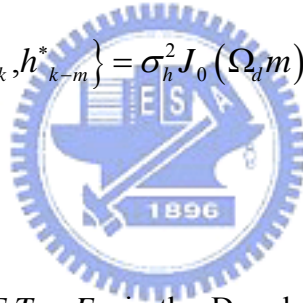
Where $\sigma_h^2 = C_h\left(0\right)$, $\Omega_d = 2\pi F_d T_s$, F_d is the Doppler spread of the fading channel, T_s is

the sample time, m is the sample index, and $J_0\left(\cdot\right)$ denotes the Bessel function of the first

kind and zero order.

Base on this assumption, we know that the channel environment has some correlation at

different times. Some channel estimators have been proposed in earlier work [[18, [24, [25,

[26]. One simple method is Pilot-Symbol-Aided Channel Estimation [18][24][25]. In a

Pilot-Symbol-Aided system, pilot symbols from a known pseudorandom-symbol sequence are

multiplexed with data symbols for transmission. The receiver has a prior knowledge of the

pilot symbol sequence and channel estimation can be facilitated with the assistance of these

known pilot symbols. The received signal can subsequently estimate and compensate for the fading effects on the data symbols. In this method, the number of pilot symbol is large. The data rate of the OFDM system is therefore not in good condition. Some other channel estimators are implemented to increase the data rate of the transmission. One direct method is Linear Interpolation channel estimation [25][26]. This scheme inserts known pilot symbols periodically both in the time and frequency dimension to track the time variation and frequency selectivity of the channel. At the receiver, the channel complex gain at the pilot symbol positions can be easily obtained from the received signal and the known pilot symbols. Interpolation is then applied to derive the estimate of the channel knowledge at data symbol positions. Pilot patterns and interpolation methods have been extensively studied in the literature. Besides linear interpolation, linear prediction is also considered as a viable approach to perform the channel estimation [15].

An important part of a receiver design is to develop accurate models for the channel as well as advanced estimation methods to estimate the model parameters. However, the system performance can also be improved by a more optimal signal design. In [15], by modeling the multipath fading channel with a complex bandpass autoregressive (AR) model, the structure of the transmitted signal is made to vary as a function of time and/or frequency according to the prevailing channel conditions. Therefore, the accurate channel modeling and advanced estimation methods are of great importance from the adaptive transmitter point of view also.

The initial channel can be obtained by these three methods, Pilot-Symbol-Aided, Linear Interpolation, and Linear Prediction. The initial channel estimate may be a sketchy channel. If

we want to obtain a more accurate channel gains, some iteration approaches can be applied. One is Low Pass Filter Fig. 3-4, the other is Expectation Maximization (EM) algorithm [16]. The EM algorithm is a technique for finding the maximum likelihood (ML) estimates of system parameters in a broad range of problems where observed data are incomplete. The EM algorithm consists of two iterative steps: the expectation (E) step and the maximization (M) step. The E-step is performed with respect to the unknown underlying parameters, using current estimates of the parameters, conditioned upon the incomplete observations. The M-step then provides new estimates of the parameters that maximize the expectation of the log-likelihood function defined over complete data, conditioned on the most recent observation and the last estimate. These two steps are iterated until the estimated values converge. The details are discussed in Chapter 3 and Chapter 4.
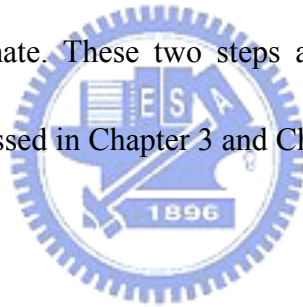
1.3 Contribution

In this thesis, several channel estimation techniques are discussed. We combine and apply them to the Orthogonal Frequency Division Multiplexing (OFDM) system. In Chapter 3, the channel environments and Decision directed Channel Estimation are introduced. We choose SUI-3, SUI-3 and Vehicular A to run the computer simulations. In Chapter 4, the Expectation Maximization algorithm based Channel Estimation is considered.

Finally, we compare and analyse the SER performance of the proposed estimators. For the result, the EM-AR can work on time and does not use any buffer to save data. The EM-Linear Interpolation can work as well as EM-AR, but it has to use some buffer, which is

not desirable in real-time applications. No mater in high speed or low speed, the Expectation

Maximization Channel Estimation can work very well.

Chapter 2

Overview of WiMAX System

2.1 Introduction to OFDM

The material in this Chapter is largely taken from [6], [7], and [13].

2.1.1 Concept and Brief Mathematical Expression of OFDM

In a single carrier system, a single fade or interference can cause the entire link to fail, but in a multicarrier system, only a small percentage of subcarriers will be affected. Error correction coding can then be used to correct for the few erroneous subcarriers. And OFDM is a special case of multicarrier transmission.

In a classical parallel data system, the total signal frequency band is divided into nonoverlapping frequency channels. It seems good to avoid spectral overlap of channels to eliminate inter-channel interference. However, this leads to inefficient use of the available spectrum. To cope with the inefficiency, the concept of using parallel data transmission by means of frequency division multiplexing (FDM) was published in mid-1960s. The concept of FDM was to use parallel data streams with overlapping carriers. The basic idea of OFDM is to divide the available spectrum into several subchannels (subcarriers). By making all subchannels narrowband, they experience almost flat fading, which makes equalization and channel estimation easier. To obtain a high spectral efficiency, the frequency response of the subchannels are overlapping and orthogonal, hence the name OFDM. This orthogonality can
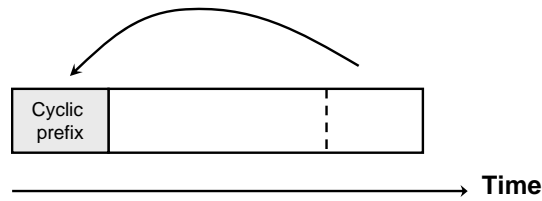
Fig. 2-1 Cyclic prefix is a copy of the last part of the OFDM symbol.

be completely maintained, even though the signal passes through a time-dispersive channel, by introducing a cyclic prefix.

A cyclic prefix is a copy of the last part of the OFDM symbol which is prepended to the transmitted symbol, see Fig. 2-1. This makes the transmitted signal periodic, which plays an important roll in avoiding intersymbol and intercarrier interference [14]. Although the cyclic prefix introduces a loss in signal-to-noise ration (SNR), it is usually a small price to pay to mitigate interference. For this system we employ the following assumptions:
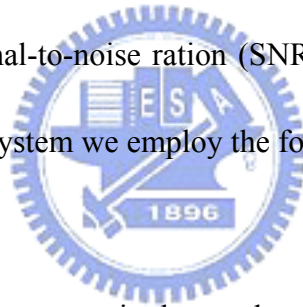
● The channel impulse response is shorter than the cyclic prefix.

● Transmitter and receiver are perfectly synchronized.

● The fading is slow enough for the channel to be considered constant during one OFDM symbol interval.

● Channel noise is additive, white, and complex Gaussian.

The brief mathematical description of the OFDM system allows us to see how the signal is generated. Mathematically, each carrier can be described as a complex wave:

$$S_c(t) = A_c(t)e^{j\left[w_c t + \phi_c(t)\right]} \qquad (2.1)$$

The real signal is the real part of $S_c(t)$. Both $A_c(t)$ and $\phi_c(t)$, the amplitude and phase of one carrier, can vary on a symbol-by-symbol basis. But the values of the parameters are constant over the symbol duration τ

An OFDM signal consists of many carriers. Thus the complex signal $S_s(t)$ can be represented as:

$$S_s(t) = \frac{1}{N}\sum_{n=0}^{N-1} A_n(t)e^{j\left[w_c t + \phi_n(t)\right]} \qquad (2.2)$$

Where $w_n = w_0 + n \triangle w$. This is a continuous-time signal. The variables $A_n(t)$ and $\phi_n(t)$ on the frequency of a particular carrier are fixed values over one symbol period, thus can be rewritten as constants:

$$A_n(t) \Rightarrow A_n$$
$$\phi_n(t) \Rightarrow \phi_n$$

If the signal is sampled with a sampling frequency of $1/T$, then the sampled signal can be represented by

$$S_s(kT) = \frac{1}{N}\sum_{n=0}^{N-1} A_n e^{j\left[(w_0 + n \triangle w)kT + \phi_n\right]} \qquad (2.3)$$

9

Besides, the symbol time is restricted to be longer than what the signal can be analyzed to N samples. It is convenient to sample over the period of one data symbol, thus

$$\tau = NT$$

To simplify the signals, let $w_0 = 0$. Then the signal becomes

$$S_s(kT) = \frac{1}{N} \sum_{n=0}^{N-1} A_n e^{j[(n\triangle w)kT + \phi_n]} \tag{2.4}$$

As we know, the form of the inverse discrete Fourier transform (IDFT) is

$$x(n) = \frac{1}{N} \sum_{k=0}^{N-1} X(w_k) e^{j\frac{2\pi kn}{N}} \tag{2.5}$$

Since the factor $A_n e^{j\phi_n}$ is constant in the sampled frequency domain (2.4) and (2.5) are equivalent if

$$\triangle f = \frac{\triangle w}{2\pi} = \frac{1}{NT} = \frac{1}{\tau} \tag{2.6}$$
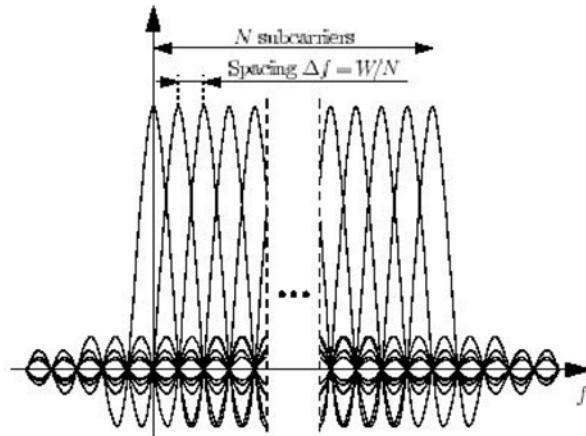
Fig. 2-2 A symbolic picture of the individual subchannels for an OFDM system with N tones over a

bandwidth W

which is equivalent to the condition for "orthogonality" discussed before. Thus as a

conclusion, using DFT to define the OFDM signal can maintain the orthogonality. Fig. 2-2

displays a schematic picture of the frequency response of the individual subchannels in an

OFDM symbol. In this figure, the individual subchannels of the system are separated and

orthogonal from each other.

2.1.2 Continous-Time Model of OFDM Including The Concept of Cyclic

The continuous-time OFDM model presented in the Fig. 2-3 can be considered as the

ideal baseband OFDM system model, which in practice is digitally synthesized and will be

discussed in the next section. We start to introduce the continuous model with the waveforms

used in the transmitter and proceed all the way to the receiver.

● **Transmitter**

Assumeing an OFDM system with N subcariers, a bandwidth of W Hz and a

symbol length of T seconds, of which T_g seconds is the length of the cyclic

| Transmitter | Channel | Receiver |
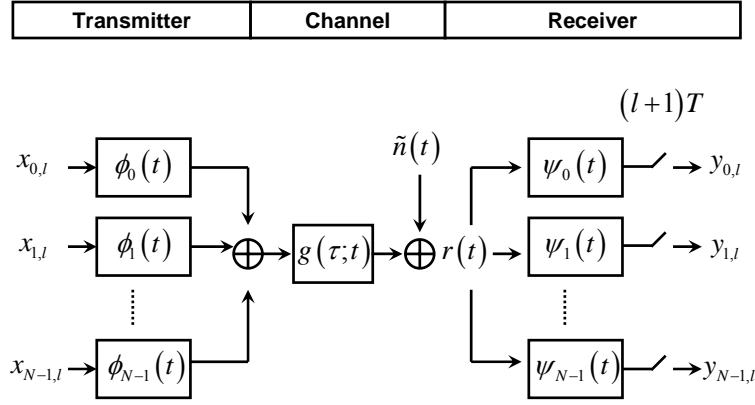
Fig. 2-3 Baseband OFDM system model

prefix, the transmitter uses the following waveforms

$$\phi_k(t) = \begin{cases} \dfrac{1}{\sqrt{T-T_g}} e^{j2\pi\frac{W}{N}k(t-T_g)} & \text{if } t \in [0,T] \\ 0, & \text{otherwise} \end{cases} \qquad (2.7)$$

Where $T = N/W + T_g$. Note that $\phi_k(t) = \phi_k(t+N/W)$ when t is within the

cyclic prefix $[0,T_g]$. Since $\phi_k(t)$ is a rectangular pulse modulated on the carrier

frequency kW/N, the common interpretation of OFDM is that it uses N

subcarriers, each carrying a low bit-rate. The waveforms $\phi_k(t)$ are used in the

modulation and the transmitted baseband signal for OFDM symbol number l as

$$s_l(t) = \sum_{k=0}^{N-1} x_{k,l} \cdot \phi_k(t-lT) \qquad (2.8)$$

Where $x_{0,l}, x_{1,l}, ..., x_{N-1,l}$, are complex numbers from a set of signal constellation

points. When an infinite sequence of OFDM symbols is transmitted, the output from

the transmitter is a juxtaposition of individual OFDM symbols as

$$s(t) = \sum_{l=-\infty}^{\infty} s_l(t) = \sum_{l=-\infty}^{\infty} \sum_{k=0}^{N-1} x_{k,l} \phi(t-lT) \qquad (2.9)$$

- **Physical channel**

We assume that the support of the (possibly time variant) impulse response $g(\tau,t)$

of the physical channel is restricted to the interval $\tau \in [0, T_g]$, i.e., to the length of

the cyclic prefix. The received signal becomes

$$r(t) = (g \times s)(t) = \int_0^{T_g} g(\tau;t) s(t-\tau) d\tau + \tilde{n}(t) \qquad (2.10)$$

Where $\tilde{n}$ is additive, white, and complex Gaussian channel noise.

- **Receiver**

The OFDM receiver consists of a filter bank, matched to the last part $[T_g, T]$ of

the transmitter waveforms $\phi_k(t)$, i.e.,

$$\psi_k(t) = \begin{cases} \phi_k^*(T-t) & \text{if } t \in [0, T-T_g], \\ 0, & \text{otherwise.} \end{cases} \qquad (2.11)$$

Effectively this means that the cyclic prefix is removed in the receiver. Since the

cyclic prefix contains all ISI from the precious symbol, the sampled output from the

13

receiver filter bank contains no ISI. Hence we can ignore the time index l when

calculating the sampled output at the th matched filter. By using (2.9), (2.10), and

(2.11), we get

$$
\begin{aligned}
y_k &= (r \times \psi_k)(t)\pi\big|_{t=T} \\
&= \int_{-\infty}^{\infty} r(t)\psi_k(T-t)\,dt \\
&= \int_{T_g}^{T}\left(\int_{0}^{T_g} g(\tau;t)\left[\sum_{k'=0}^{N-1} x_{k'}\phi_{k'}(t-\tau) \right]d\tau \right)\phi_k^*(t)\,dt \\
&\quad + \int_{T_g}^{T} \tilde{n}(T-t)\phi_k^*(t)\,dt
\end{aligned}
\tag{2.12}
$$

We consider the channel to be fixed over the OFDM symbol interval and denote it

by $g(\tau)$, which gives

$$
y_k = \sum_{k'=0}^{N-1} \int_{T_g}^{T}\left(\int_{0}^{T_g} g(\tau)\phi_{k'}(t-\tau)\,d\tau \right)\phi_k^*(t)\,dt + \int_{T_g}^{T}\tilde{n}(T-t)\phi_k^*(t)\,dt
\tag{2.13}
$$

The integration intervals are $T_g < t < T$ and $0 < \tau < T_g$, which implies that

$0 < t - \tau < T$ and the inner integral can be written as

$$
\begin{aligned}
&\int_{0}^{T_g} g(\tau)\phi_{k'}(t-\tau)\,d\tau \\
&= \int_{0}^{T_g} g(\tau)\frac{e^{j2\pi k'(t-\tau-T_g)W/N}}{\sqrt{T-T_g}}\,d\tau \\
&= \frac{e^{j2\pi k'(t-T_g)W/N}}{\sqrt{T-T_g}}\int_{0}^{T_g} g(\tau)e^{-j2\pi k'\tau W/N}\,d\tau \quad T_g < t < T
\end{aligned}
\tag{2.14}
$$

14

The latter part of this expression is the sampled frequency response of the channel

at frequency $f = k'W/N$, i.e., at the k th subcarrier frequency:

$$h_{k'} = G\left(k'\frac{W}{N}\right) = \int_0^{T_g} g(\tau)e^{-j2\pi k'\tau W/N}d\tau \qquad (2.15)$$

Where $G(f)$ is the Fourier transform of $g(\tau)$. Using this notation, the output

from the receiver filter bank can be simplified to

$$
\begin{aligned}
y_k \\
&= \sum_{k'=0}^{N-1} x_{k'} \int_{T_g}^{T} \frac{e^{j2\pi k'(t-T_g)W/N}}{\sqrt{T-T_g}} h_{k'}\phi_k^*(t)dt + \int_{T_g}^{T} \tilde{n}(T-t)\phi_k^*(t)dt \\
&= \sum_{k'=0}^{N-1} x_{k'}h_{k'} \int_{T_g}^{T} \phi_{k'}(t)\phi_k^*(t)dt + n_k
\end{aligned}
\qquad (2.16),
$$

where $n_k = \int_{T_g}^{T} \tilde{n}(T-t)\phi_k^*(t)dt$. Since the transmitter filters $\phi_k(t)$ are orthogonal,

the following equation is thus obtained.

$$
\begin{aligned}
&\int_{T_g}^{T} \phi_{k'}(t)\phi_{k'}^*(t)dt \\
&= \int_{T_g}^{T} \frac{e^{j2\pi k'(t-T_g)W/N}}{\sqrt{T-T_g}} \frac{e^{-j2\pi k(t-T_g)W/N}}{\sqrt{T-T_g}} dt = \delta[k-k']
\end{aligned}
\qquad (2.17)
$$

According to (2.16), we know that

$$y_k = h_k + n_k \qquad (2.18)$$
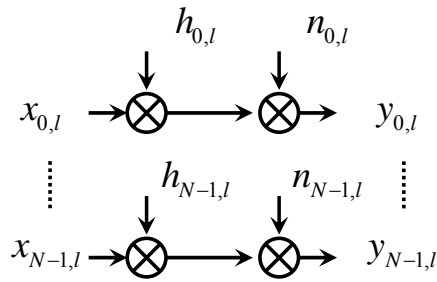
Fig. 2-4 Continuous-time OFDM system interpreted as parallel Gaussian channels.

The benefit of a cyclic prefix is twofold: it avoids both ISI (since it acts as a guard space) and ICI (since it maintains the orthogonality of the subcarriers). By re-introducing the time index l, we may now view the OFDM system as a set of parallel Gaussian channels, according to Fig. 2-4.

2.1.3 Discrete-Time Model

An entirely discrete-time model of and OFDM systme is displayed in Fig. 2-5. Compared to the continous-time model, the modulation and demodulation are replaced by an inverse DFT (IDFT) and a DFT respectively and the channel is a discrete-time convolution. The cyclic prefix operates in the same fashion in this system and the calculations can be performed in essentially the same way. The main difference is that all integrals are replaced by sums.
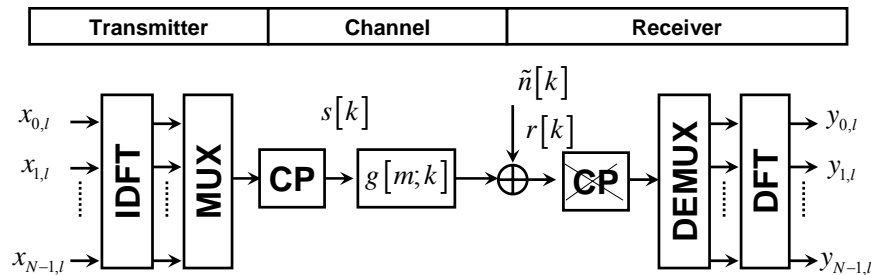
Fig. 2-5 Discrete-time OFDM system

As far as the receiver is concerned, the use of a cyclic prefix longer than the channel

response will transform the linear convolution in the channel into a cyclic convolution.

Denoting cyclic convolution by "$\otimes$", we can write the whole OFDM system as

$$y_l = DFT\left(IDFT\left(x_1\right)\otimes g_1 + \tilde{n}_1\right)$$
$$= DFT\left(IDFT\left(x_1\right)\otimes g_1\right) + n_1 \qquad (2.19)$$

Where y_1 contains the N received data points, x_1 is the N transmitted constellation

points, g is the channel impulse response of the channel (padded with zeros to obtain a

length of N), and $\tilde{n}_1$ is the channel noise. Since the channel noise is assumed to be white

Gaussian, the term $n_1 = DFT\left(\tilde{n}_1\right)$ represents uncorrelated Gaussian noise. Furthermore, we

use the fact that the DFT of two cyclically convolved signals is equivalent to the product of

their individual DFTs. Denoting element-by-element multiplication by "$\bullet$", the above

expression can thus be written as

$$y_1 = x_1 \bullet DFT\left(g_1\right) + n_1 = x_1 \bullet h_1 + n_1 \qquad (2.20)$$

Where $h_1 = DFT\left(g_1\right)$ is the frequency response of the channel. Therefore we have

obtained the same type of parallel Gaussian channels as the continuous-time model. The only

difference is that the channel attenuations h_1 are given by the N-point DFT of the

discrete-time channel, instead of the sampled frequency response as in (2.15).

2.1.4 Imperfections of OFDM

Depending on the mathematical analyzed situation disscused before, imperfections in a real OFDM system may be ignored or explicitly included in the model. Below we mention of the imperfections and their corresponding effects.

- **Dispersion**

  Both time and frequency dispersion of the channel can destroy the orthogonality of the system, i.e., introduce both ISI and ICI. If these effects are not sufficiently mitigated by e.g., a cyclic prefix and a large inter-carrier spacing, they have to be included in the model. One way of modelling these effects is an increase of the additive noise.

- **Nonlinearities and clipping distortion**

  OFDM systems have high peak-to-average power ratios and high demands on linear amplifiers. Nonlinearities in amplifiers may cause both ISI and ICI in the system. Especially, if the amplifiers are not designed with proper output back-off (OBO), the clipping distortion may cause severe degradation.

- **External interference**

  In wireless systems, the external interference usually stems from radio transmitters and other types of electronic equipment in the vinciniy of the receiver.

2.2 Introduction to OFDMA

OFDMA is a multiple access method based on OFDM signaling that allows simultaneous

Table 2-1 OFDM Advantages and Disadvantages

Advantages	Disadvantages
Bandwidth efficiency	Sensitive to frequency offset
Immunity to multipath effect	Sensitive to timing offset
Robust against narrowband interference	Sensitive to phase noise
	Large peak-to-average power ratio

transmissions to and from multiple users along with the other advantages of OFDM. In OFDM, a channel is divided into carriers which is used by one user at any time. In OFDMA, the carriers are divided into subchannels. Each subchannel has multiple carriers that form one unit in frequency allocation. In this way, the bandwidth can be allocated dynamically to the users according to their needs. A simple comparison of the subcarrier allocation of OFDM
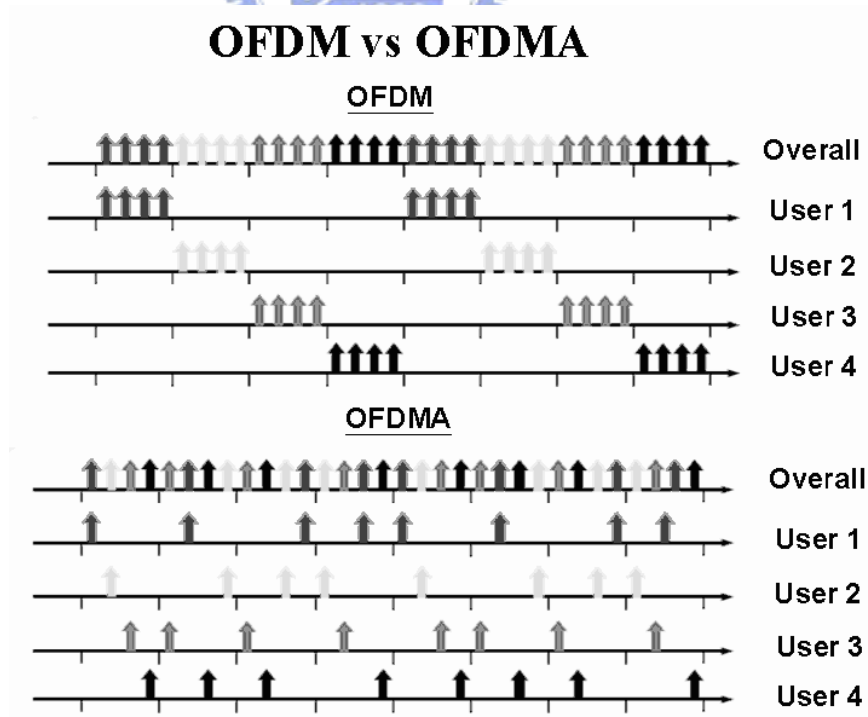
Fig. 2-6 Comparison of subcarrier allocatins in OFDM and OFDMA (from [8]).

and OFDMA is shown in Fig. 2-6.

An additional advantage of OFDMA is the following. Due to the large variance in a mobile system's path loss, inter-cell interference is a common issue in mobile wireless systems. An OFDMA system can be designed such that subchannels can be composed from several distinct permutations of subcarriers. This enables significant reduction in inter-cell interference when the system is not fully loaded, because even on occasions where the same subchannel is used at the same time in two different cells, there is only a partial collision on
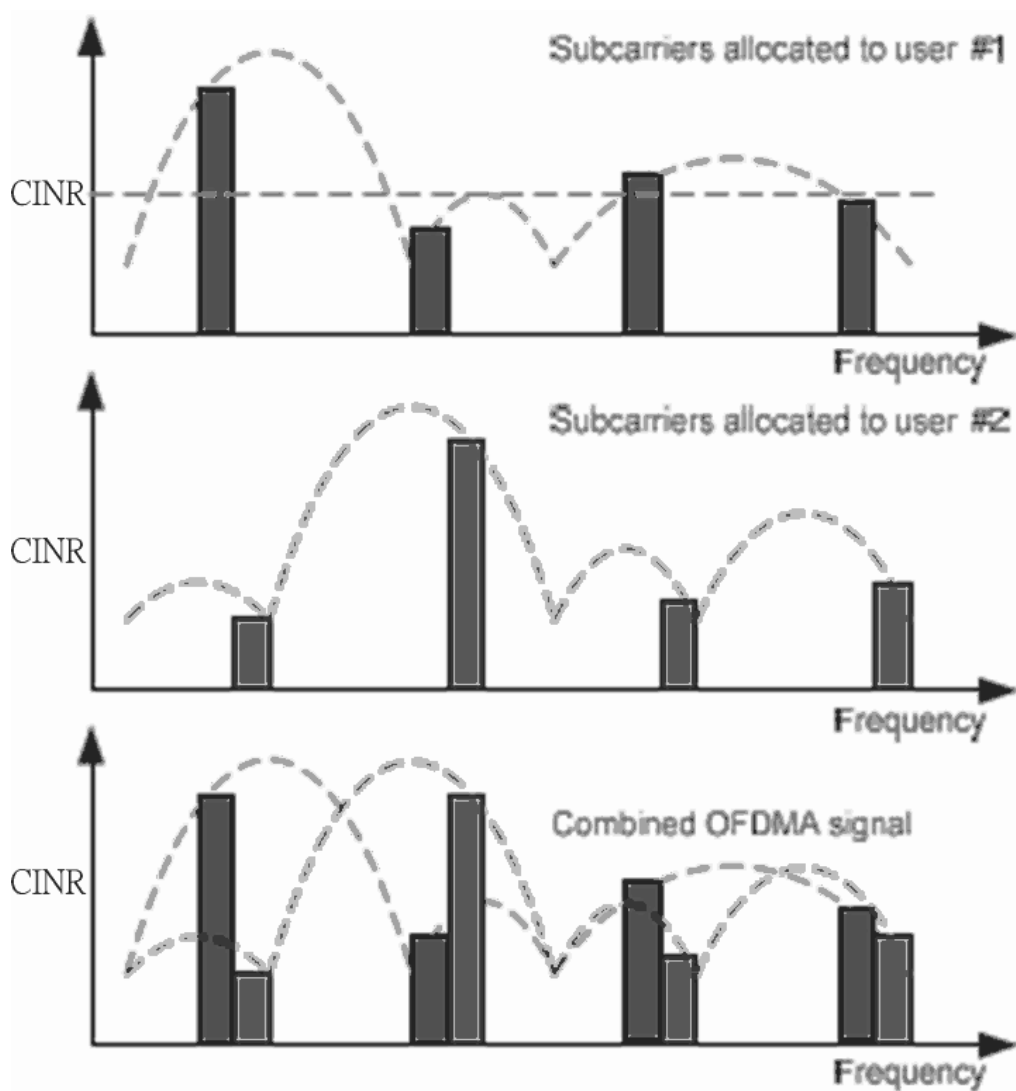
Fig. 2-7 Subcarrier allocation in an OFDMA symbol (from [9]).

the active sub-carriers.

Fig. 2-7 shows an example subcarrier allocation in an OFDMA symbol. The frequency response of a typical broadband wireless channel is also depicted. In this example, the deep-fading condition and narrowband interference are considered. In the top plot, we see that when the channel is in deep fade, the subcarriers are not sufficiently energy efficient to carry information. These wasted subcarriers can be utilized by there uses in OFDMA, thus achieving higher efficiency and capacity. Very few, if any, subcarriers are likely to be wasted in OFDMA, since no particular subcarrier is likely to be bad for all users.

In order to support multiple users, the control mechanism becomes more complex. Besides, the OFDMA system has some implementation issues which are more complicated to handle. For example, power control is needed for the uplink to make signals from different users have equal power at the receiver, and all users have to adjust their transmitting time to be aligned. We shall address some issues in the context of IEEE 802.16e.

2.3 Introduction to IEEE 802.16e

Since the publication of the IEEE 802.16 standard for fixed broadband wireless access in 2001, a number of revision and amendments have taken place. Like other IEEE 802 standards, the 802.16 standards are primarily concerned with physical (PHY) layer and medium access control (MAC) layer functionalities. The idea originally was to provide broadband wireless access to buildings through external antennas communicating with radio base stations (BSs).

To overcome the disadvantage of the line-of-sight (LOS) requirement between

transmitters and receivers in the 802.16 standard, the 802.16a standard was approved in 2003 to support nonline-of-sight (NLOS) links, operational in both licensed and unlicensed frequency bands from 2 to 11 GHz, and subsequently revised to create the 802.16d standard (now code-named 802.16-2004). With such enhancements, the 802.16-2004 standard has been viewed as a promising alternative for providing the last-mile connectivity by radio link. However, the 802.16-2004 specifications were devised primarily for fixed wireless users. The 802.16e task group was subsequently formed with the goal of extending the 802.16-2004 standard to support mobile terminals.

The IEEE 802.16e has been published in Febuary 2006. It specifies four air interfaces: WirelessMAN-SC PHY, WirelessMAN-SCa PHY, WirelessMAN-OFDM PHY, and WirelessMAN-OFDMA PHY. This study is concerned with WirelessMAN-OFDMA PHY in a mobile communication environment.
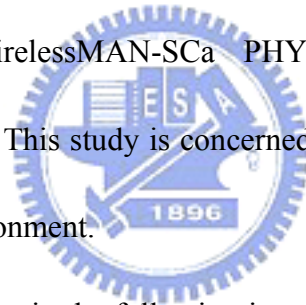
Some glossary we will often use in the following is as follows. The direction of transmission from the base station (BS) to the subscriber station (SS) is called downlink (DL), and the opposite direction is uplink (UL). The SS is considered synonymous as the mobile station (MS). It is sometimes termed the user. The BS is a generalized equipment set providing connectivity, management, and control of the SS.

2.3.1 OFDMA Basic Terms

In the OFDMA mode, the active subcarriers are divided into subsets of subcarriers, where each subset is termed a subchannel. The subcarriers forming one subchannel may, but need
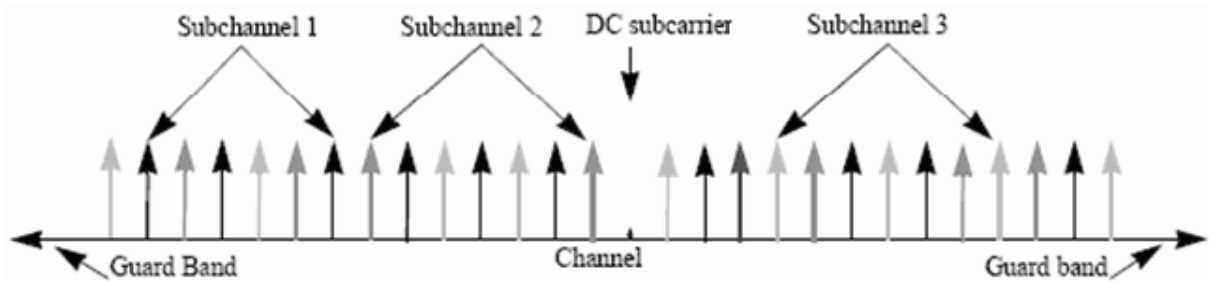
Fig. 2-8 OFDMA frequency description (3-channel schematic example, from [4]).

not be, adjacent. The concept is shown in Fig. 2-8.

Three basic types subchannel organization are defined: partial usage of subchannels (PUSC), full usage of subchannels (FUSC), and adaptive modulation and coding (AMC); among which the PUSC is mandatory and the other two are optional. In PUSC DL, the entire channel bandwidth is divided into three segments to be used separately. The FUSC is employed only in the DL and it uses the full set of available subcarriers so as to maximize the throughput.

Slot and Data Region

The definition of an OFDMA slot depends on the OFDMA symbol structure, which varies for uplink and downlink, for FUSC and PUSC, and for the distributed subcarrier permutations and the adjacent subcarrier permutation.

- For downlink PUSC using the distributed subcarrier permutation, one slot is one subchannel by two OFDMA symbols.

- For uplink PUSC using either of the distributed subcarrier permutations, one slot is one subchannel by three OFDMA symbols.

- For downlink FUSC and downlink optional FUSC using the distributed subcarrier permutation, one slot is one subchannel by one OFDMA symbol.

In OFDMA, a data region is a two-dimensional allocation of a group of contiguous

23
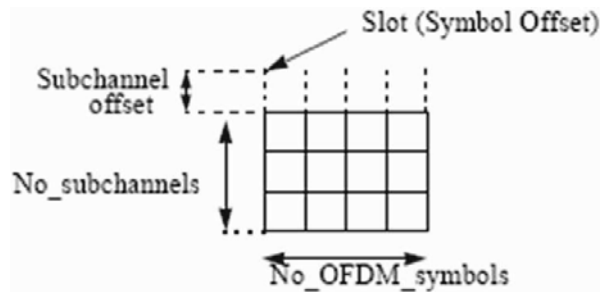
Fig. 2-9 Example of the data region which defines the OFDMA allocation (from [4]).

subchannels, in a group of contiguous OFDMA symbols. All the allocations refer to logical

subchannels. This two-dimensional allocation may be visualized as a rectangle, such as the

4×3 rectangle shown in Fig. 2-9

Segment

A segment is a subdivision of the set of available OFDMA subchannels (that may include all

available subchannels). One segment is used for deploying a single instance of the MAC.

Permutation Zone

A permutation zone is a number of contiguous OFDMA symbols, in the DL or the UL, that

use the same permutation formula. The DL subframe or the UL subframe may contain more

than one permutation zone. The concept of permutation zone will be further elaborate later.

2.3.2 OFDMA Symbol Parameters

- Some OFDMA symbol parameters are listed below.

- BW : Nominal channel bandwidth.

- N_{used} : Number of used subcarriers.

- n : Sampling factor. This parameter, in conjunction with BW and N_{used},

  determines the subcarrier spacing and the useful symbol time.

- G : Ratio of cyclic prefix (CP) time to useful time.

- N_{FFT} : Smallest power of two greater than N_{used}.

- Sampling frequency: $F_s = \lceil n \cdot BW/8000 \rceil \times 800$.

- Subcarrier spacing: $\Delta f = F_s / N_{FFT}$.

- Useful symbol time: $T_b = 1/\Delta f$.

- Cyclic prefix (CP) time: $T_g = G \cdot T_b$.

- OFDM symbol time: $T_s = T_b + T_g$.

- Sampling time: T_b / N_{FFT}.

2.3.3 Scalable OFDMA [9]

One feature of the IEEE 802.16e OFDMA is the selectable FFT size, from 128 to 2048 in multiples of 2, excluding 256 to be used with OFDM. This has been termed scalable OFDMA (S-OFDMA). One use of S-OFDMA is that if the channel bandwidths are allocated based on integer power of 2 times a base bandwidth, then one may consider making the FFT size proportional to the allocated bandwidth so that all systems are based on the same subcarrier spacing and the same OFDMA symbol duration, which may simplify system design. For example, Table 2-2 lists some S-OFDMA parameters proposed by the WiMAX Forum [10]. S-OFDMA supports a wide range of bandwidth to flexibly address the need for various spectrum allocation and usage model requirements.

When designing OFDMA wireless systems the optimal choice of the number of subcarriers per channel bandwidth is a tradeoff between protection against multipath, Doppler shift, and design cost/coplexity. Increasing the number of subcarriers leads to better immunity to the ISI

Table 2-2 S–OFDMA Parameters Proposed by WiMAX Forum

Parameters	Values			
System Channel Bandwidth (MHz)	1.25	5	10	20
Sampling Frequency (MHz)	1.4	5.6	11.2	22.4
FFT Size	128	512	1024	2048
Subcarrier Spacing (Δf)	10.94 kHz			
Useful Symbol Time ($T_b = 1/\Delta f$)	91.4 μ sec			
Guard Time ($T_g = T_b/8$)	11.4 μ sec			
OFDMA Symbol Duration ($T_s = T_b + T_g$)	102.9 μ sec			

caused by multipath; on the other hand it increases the cost and complexity of the system (it leads to higher requirements for signal processing power and power amplifiers with the capability of handling higher peak-to-average power ratios). Having more subcarriers also results in narrower subcarrier spacing and therefore the system becomes more sensitive to Doppler shift and phase noise. Calculations show that the optimum tradeoff for mobile systems is achieved when subcarrier spacing is about 11 kHz [11] .

2.4 OFDMA Frame Structure

Duplexing Modes

In licensed bands, the duplexing method shall be either frequency-division duplex (FDD) or time-division duplex(TDD). FDD SSs may be half-duplex FDD (H-FDD). In license exempt bands, the duplexing method shall be TDD.

Point-to-Multipoint (PMP) Frame Structure

When implementing a TDD system, the frame is composed of BS and SS transmissions. Fig. 2-10 shows an example. Each frame in the downlink transmission begins with a preamble
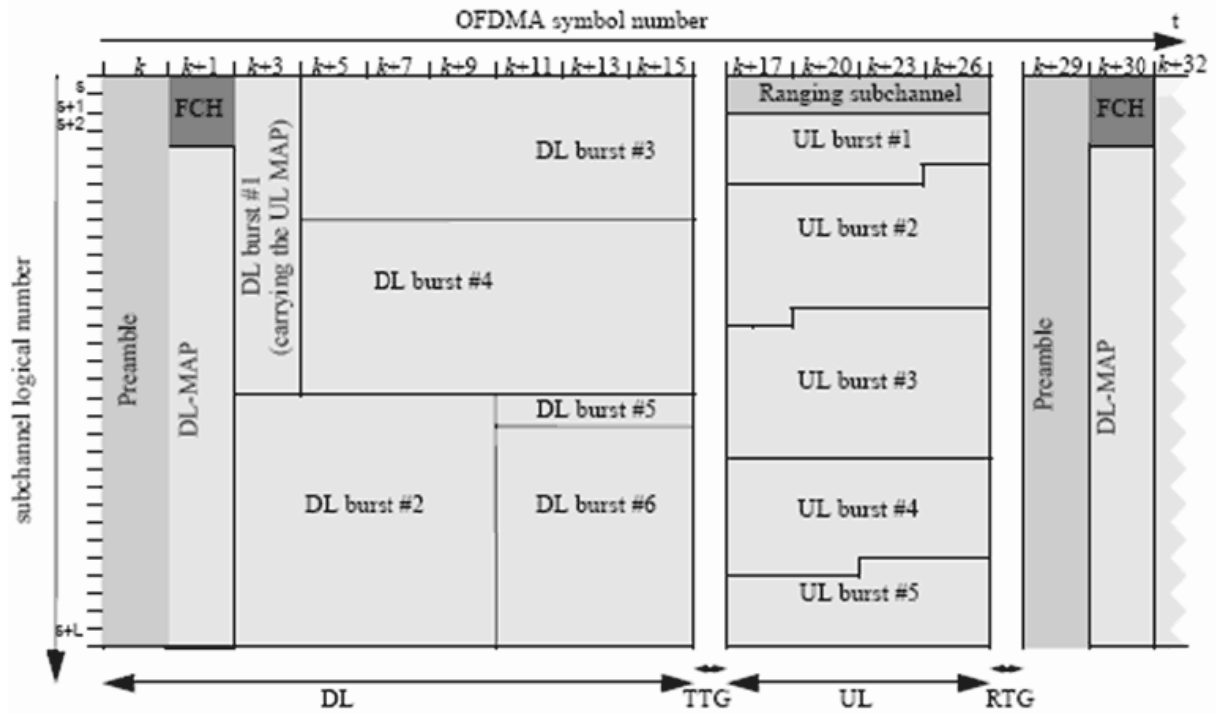
Fig. 2-10 Example of an OFDMA frame (with only mandatory zone) in TDD mode (from [2]).

followed by a DL transmission period and an UL transmission period. In each frame, time

gaps, denoted transmit/receive transition gap (TTG) and receive/transmit gap (RTG), are

between the downlink and uplink subframes and at the end of each frame, respectively placed.

They allow transitions between transmission and reception functions.

Subchannel allocation in the downlink may be performed with PUSC where some of the

subchannels are allocated to the transmitter or FUSC where all subchannels are allocated to

the transmitter. The downlink frame shall start in PUSC mode with no transmit diversity. The

FCH shall be transmitted using QPSK rate 1/2 with four repetitions using the mandatory

coding scheme (i.e., the FCH information will be sent on four subchannels with successive

logical subchannel numbers) in a PUSC zone. The FCH contains the DL Frame Prefix which

specifies the length of the DL-MAP message that immediately follows the DL Frame Prefix
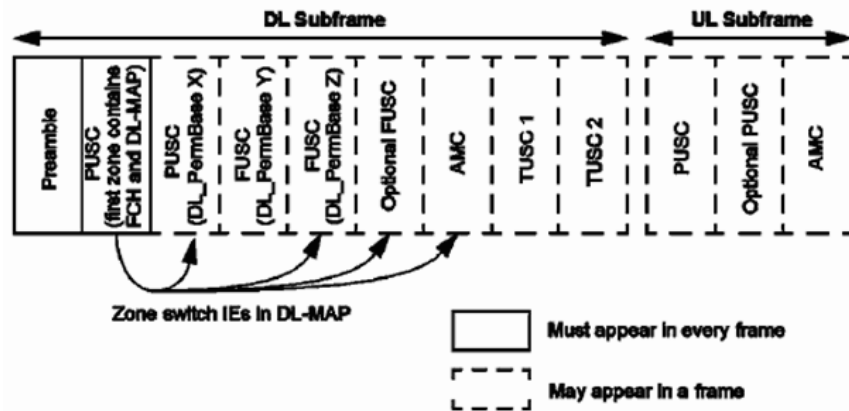
Fig. 2-11 Illustration of OFDMA with multiple zones (from [2]).

and the repetition coding used for the DL-MAP message.

The transitions between modulations and coding take place on slot boundaries in time domain (except in AAS zone, where AAS stands for adaptive antenna system) and on subchannels within an OFDMA symbol in frequency domain. The OFDMA frame may include multiple zones (such as PUSC, FUSC, PUSC with all subchannels, optional FUSC, AMC, TUSC1, and TUSC2, where AMC stands for adaptive modulation and coding, and TUSC stands for tile usage of subchannels), the transition between zones is indicated in the DL-Map. Fig. 2-11 depicts an OFDMA frame with multiple zones.

The PHY parameters (such as channel state and interference levels) may change from one zone to the next.

The maximum number of downlink zones is 8 in one downlink subframe. For each SS, the maximum number of bursts to decode in one downlink subframe is 64. This includes all bursts without connection identifier (CID) or with CIDs matching the SS's CIDs.

Allocation of Subchannels for FCH and DL-MAP, and Logical Subchannel Numbering

In PUSC, any segment used shall be allocated at least the same number of subchannels as in
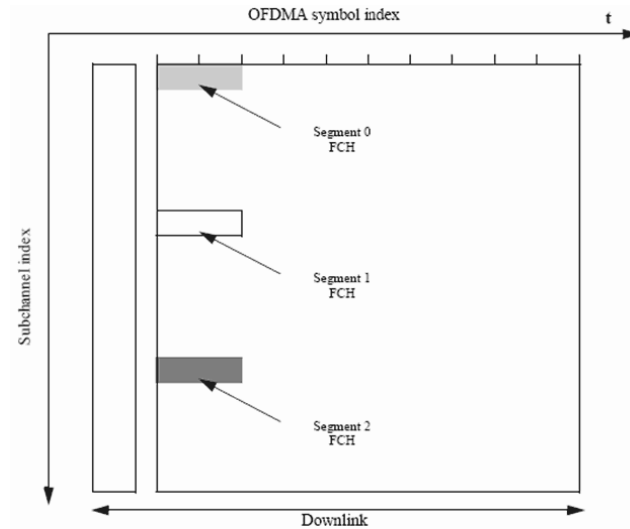
Fig. 2-12 FCH subchannel allocation for all 3 segments (from [4]).

subchannel group #0. For FFT sizes other than 128, the first 4 slots in the downlink part of the

segment contain the FCH as defined before. These slots contain 48 bits modulated by QPSK

with coding rate 1/2 and repetition coding of 4. For FFT-128, the first slot in the downlink

part of the segment is dedicated to FCH and repetition is not applied. The basic allocated

subchannel sets for segments 0, 1, and 2 are subchannel groups #0, #2, and #4, respectively.

Fig. 2-12 depicts this structure.

After decoding the DL Frame Prefix message within the FCH, the SS has the knowledge of

how many and which subchannels are allocated to the PUSC segment. In order to observe the

allocation of the subchannels in the downlink as a contiguous allocation block, the

subchannels shall be renumbered. The renumbering, for the first PUSC zone, shall start from

the FCH subchannels (renumbered to values 0–11), then continue numbering the subchannels

in a cyclic manner to the last allocated subchannel and from the first allocated subchannel to

the FCH subchannels. Fig. 2-13 gives an example of such renumbering for segment 1.
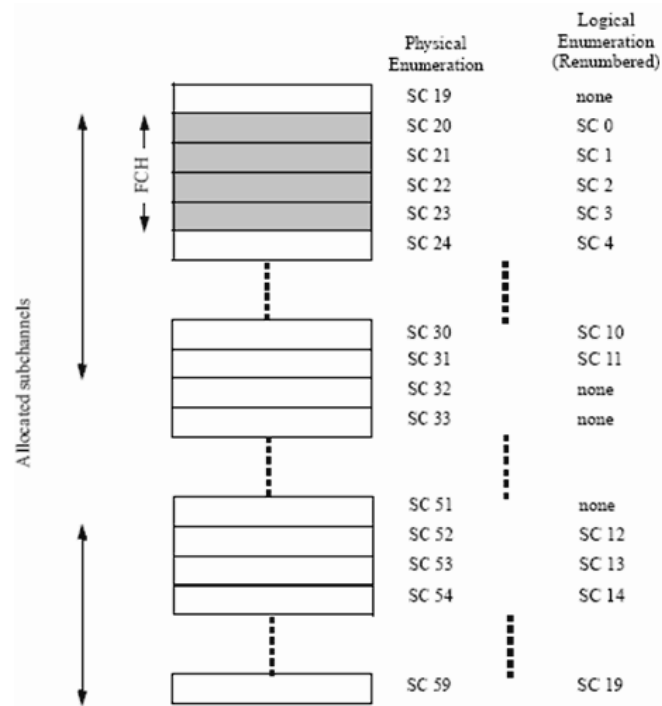
Fig. 2-13 Example of DL renumbering the allocated subchannels for segment 1 in PUSC(from [4]).

For uplink, in order to observe the allocation of the subchannels as a contiguous allocation block, the subchannels shall be renumbered, and the renumbering shall start from the lowest numbered allocated subchannel (renumbered to value 0), up to the highest numbered allocated subchannel, skipping nonallocated subchannels.

The DL-MAP of each segment shall be mapped to the slots allocated to the segment in a frequency first order, starting from the slot after the FCH (subchannel 4 in the first symbol, after renumbering), and continuing to the next symbols if necessary. The FCH of segments that have no subchannels allocated (unused segments) will not be transmitted, and the respective slots may be used for transmission of MAP and data of other segments.

2.5 OFDMA Subcarrier Allocation

As mentioned, the OFDMA PHY defines four scalable FFT sizes: 2048, 1024, 512, and 128.

For convenience, here we only take the 1024-FFT OFDMA subcarrier allocation for introduction. The subcarriers are divided into three types: null (guard band and DC), pilot, and data. Subtracting the guard tones from N_{FFT}, one obtains the set of "used" subcarriers N_{used}. For both uplink and downlink, these used subcarriers are allocated to pilot subcarriers and data subcarriers. However, there is a difference between the different possible zones. For FUSC and PUSC, in the downlink, the pilot tones are allocated first; what remains are data subcarriers, which are divided into subchannels that are used exclusively for data. Thus, in FUSC, there is one set of common pilot subcarriers, and in PUSC downlink, there is one set of common pilot subcarriers in each major group, but in PUSC uplink, each subchannel contains its own pilot subcarriers.

2.5.1 Downlink

Preamble

The first symbol of the downlink transmission is the preamble. There are three types of preamble carrier-sets, which are defined by allocation of different subcarriers for each one of them. The subcarriers are modulated using a boosted BPSK modulation with a specific pseudo-noise (PN) code. The preamble carrier-sets are defined using

$$PreambleCarrierSet_n = n + 3 \cdot k \qquad (2.21)$$

Where :

$PreambleCarrierSet_n$ specifies all subcarriers allocated to the specific preamble,

n is the number of the preamble carrier-set indexed 0–2,

k is a running index 0–283.

For the preamble symbol there are 86 guard band subcarriers on the left side and the right side of the spectrum. Each segment uses a preamble composed of a carrier-set out of the three available carrier-sets in the manner that segment i uses preamble carrier-set i, where $i = 0, 1, 2$. Therefore, each segment eventually modulates each third subcarrier. In the case of segment 0, the DC carrier will be zeroed and the corresponding PN number will be discarded.

The 114 different PN series modulating the preamble carrier-set are defined in Table 309 of [4] for the 1024-FFT mode. The series modulated depends on the segment used and the IDcell parameter.

Symbol Structure for PUSC

The symbol is first divided into basic clusters and zero carriers are allocated. Pilots and data carriers are allocated within each cluster. Table 310 of [2] summarizes the parameters of the symbol structure of different FFT sizes for PUSC mode. Here we only take the 1024-FFT OFDMA downlink carrier allocation for example, which is summarized in Table 2-3. Fig. 2-14 depicts the DL cluster structure.

Downlink Subchannels Subcarrier Allocation in PUSC

The subcarrier allocation to subchannels is performed using the following procedure:

1. Dividing the subcarriers into the number of clusters ($N_{clusters}$), where the physical clusters
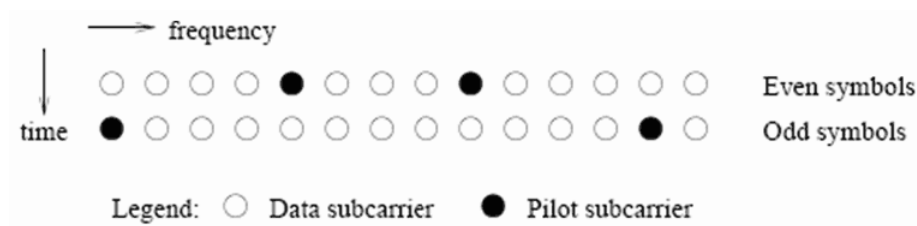
Fig. 2-14 DL cluster structure (from [12]).

Table 2-3 1024-FFT OFDMA DL Carrier Allocation for PUSC

Parameter	Value	Comments
Number of DC subcarriers	1	Index 512
Number of guard subcarriers, left	92	
Number of guard subcarriers, right	91	
Number of used subcarriers, N_{used}	841	
Renumbering sequence	6, 48, 37, 21, 31, 40, 42, 56, 32, 47, 30, 33, 54, 18, 10, 15, 50, 51, 58, 46, 23, 45, 16, 57, 39, 35, 7, 55, 25, 59, 53, 11, 22, 38, 28, 19, 17, 3, 27, 12, 29, 26, 5, 41, 49, 44, 9, 8, 1, 13, 36, 14, 43, 2, 20, 24, 52,4, 34, 0	Used to renumber clusters before allocation to subchannels.
Number of subcarriers per cluster	14	
Number of clusters	60	
Number of data subcarriers in each symbol per subchannel	24	
Number of subchannels	30	
Basic permutation sequence 6 (for 6 subchannels)	3, 2, 0, 4, 5, 1	
Basic permutation sequence 4 (for 4 subchannels)	3, 0, 2, 1	

contain 14 adjacent subcarriers each (starting from carrier 0). The number of clusters

varies with the FFT size.

2. Renumbering the physical clusters into logical clusters using the following formula:

$$LogicalCluster=$$

$$\begin{cases} RenumberingSequence(PhysicalCluster), & \text{first DL zone, or Use All SC indicator} \\ & = 0 \text{ in STC DL Zone IE,} \\ \\ RenumberingSequence((PhysicalCluster)+ & \text{otherwise.} \\ 13 \cdot DL\, PermBase)mod N_{clusters} \end{cases} \quad (2.22)$$

In the first PUSC zone of the downlink (first downlink zone) and in a PUSC zone defined by STC DL ZONE IE() with "use all SC indicator = 0", the default renumbering sequence is used for logical cluster definition. For all other cases DL PermBase parameter in the STC DL Zone IE() or AAS DL IE() shall be used.

3. Allocating logical clusters to groups. The allocation algorithm varies with FFT size. For FFT size = 1024, dividing the clusters into six major groups. Group 0 includes clusters 0–11, group 1 clusters 12–19, group 2 clusters 20–31, group 3 clusters 32–39, group 4 clusters 40–51, and group 5 clusters 52–59. These groups may be allocated to segments; if a segment is used, then at least one group shall be allocated to it. By default group 0 is allocated to sector 0, group 2 to sector 1, and group 4 to sector 2.

4. Allocating subcarriers to subchannels in each major group, which is performed separately for each OFDMA symbol by first allocating the pilot carriers within each cluster, and then partitioning all remaining data carriers into groups of contiguous subcarriers. Each subchannel consists of one subcarrier from each of these groups. The number of groups is therefore equal to the number of subcarriers per subchannel, and it is denoted $N_{subcarriers}$. The number of the subcarriers in a group is equal to the number of subchannels, and it is denoted $N_{subchannels}$. The number of data subcarriers is thus equal to $N_{subcarriers} \cdot N_{subchannels}$. The parameters vary with FFT sizes. For FFT size = 1024, use the

parameters from Table 2-3, with basic permutation sequence 6 for even numbered major groups and basic permutation sequence 4 for odd numbered major groups, to partition the subcarriers into subchannels containing 24 data subcarriers in each symbol. The exact partitioning into subchannels is according to the permutation formula:

$$subcarrier(k,s) = N_{subchannels} \cdot n_k$$
$$+ \{p_s[n_k \bmod N_{subchannels}] + DL\_PermBase\} \bmod N_{subchannels}$$

(2.23)

where:

$subcarrier(k,s)$ is the subcarrier index of subcarrier k in subchannel s,

s is the index number of a subchannel, from the set $\{0,...,N_{subchannels}-1\}$,

n_k $= (k+13 \cdot s) \bmod N_{subchannels}$ where k is the subcarrier-in-subchannel index from the set $\{0,...,N_{subchannels}-1\}$,

$N_{subchannels}$ is the number of subchannels (for PUSC use number of subchannels in the currently partitioned major group),

$p_s[j]$ is the series obtained by rotating basic permutation sequence cyclically to the left s times,

$DL\_PermBase$ is an integer ranging from 0 to 31, which is set to the preamble IDCell in the first zone and determined by the DL-MAP for other zones.

On initialization, an SS must search for the downlink preamble. After finding the preamble, the user shall know the IDcell used for the data subchannels.

2.5.2 Uplink

The UL follows the DL model, therefore it also supports up to three segments. The UL

Table 2-4 1024-FFT OFDMA UL Carrier Allocation for PUSC

Parameter	Value	Comments
Number of DC subcarriers	1	Index 512
N$_{used}$	841	
Guard subcarriers: left, right	92,91	
TilePermutation	11, 19, 12, 32, 33, 9, 30, 7, 4, 2, 13, 8, 17, 23, 27, 5, 15, 34, 22, 14, 21, 1, 0, 24, 3, 26, 29, 31, 20, 25, 16, 10, 6, 28, 18	used to allocate tiles to subchannels
N$_{subchannels}$	35	
N$_{tiles}$	210	
Tile per subchannel	6	

supports 35 subchannels where each transmission uses 48 data subcarriers as the minimal

block of processing. Each new transmission for the uplink commences with the parameters as

given in Table 2-4.
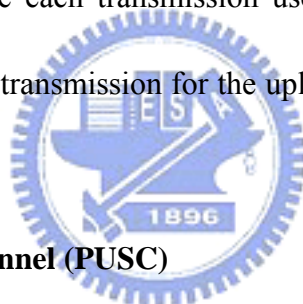
Symbol Structure for Subchannel (PUSC)

A slot in the uplink is composed of three OFDMA symbols and one subchannel. Within each

slot, there are 48 data subcarriers and 24 fixed-location pilots. The subchannel is constructed

from six uplink tiles, each tile has four successive active subcarriers and its configuration is

illustrated in Fig. 2-15 .

Fig. 2-15 Description of an UL tile (from [12]).

Partitioning of Subcarriers into Subchannels in the Uplink

The usable subcarriers in the allocated frequency band shall be divided into N_{tiles} physical

tiles as defined in Fig. 2-15 with parameters from Table 2-4. The allocation of physical tiles to

logical tiles in subchannels is performed in the following manner:

$$Tiles(s,n) = N_{subchannels} \cdot n_k \\ + \left\{ p_t \left[(s+n) \bmod N_{subchannels} \right] + UL\_PermBase \right\} \bmod N_{subchannels}$$

(2.24)

where:

$Tiles(s,n)$ is the physical tile index in the FFT with tiles being ordered consecutively

from the most negative to the most positive used subcarrier (0 is the

starting tile index),

n is the tile index 0,...,5 in a subchannel,

p_t is the tile permutation,

$N_{subchannels}$ is the number of subchannels,

s is the subchannel number in the range $\left\{ 0,..., N_{subchannels} - 1 \right\}$

$UL\_PermBase$ is an integer value in the range 0:::69, which is assigned by a

management entity.

After mapping the physical tiles in the FFT to logical tiles for each subchannel, the data

subcarriers per slot are enumerated by the following process:

1. After allocating the pilot carriers within each tile, indexing of the data subcarriers within

each slot is performed starting from the first symbol at the lowest indexed subcarrier of

the lowest indexed tile and continuing in an ascending manner through the subcarriers in the same symbol, then going to the next symbol at the lowest indexed data subcarrier, and so on. Data subcarriers shall be indexed from 0 to 47.

2. The mapping of data onto the subcarriers will follow (2.25), which calculates the subcarrier index (as assigned in item 1) to which the data constellation point is to be mapped:

$$Subcarriers(n,s) = (n+13\cdot s)\bmod N_{subchannels} \qquad (2.25)$$

where:

$Subcarriers(n,s)$ is the permutated subcarrier index corresponding to data subcarrier n is subchannel s,

n is the running index 0,...,47, indicating the data constellation point,

s is the subchannel number,

$N_{subchannels}$ is the number of subcarriers per slot.
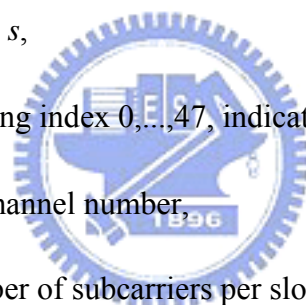
2.6 Modulation

Subcarrier Randomization

The pseudo random binary sequence (PRBS) generator, as shown in Fig. 2-16, shall be used to produce a sequence w_k. The polynomial for the PRBS generator shall be $X^{11} + X^9 + 1$. The value of the pilot modulation on subcarrier k shall be derived from w_k.

The initialization vector of the PRBS generator for both uplink and downlink, designated b10..b0, is defined as follows:

b0..b4 = five least significant bits of IDcell as indicated by the frame preamble in the first downlink zone and in the downlink AAS zone with Diversity Map support, DL PermBase
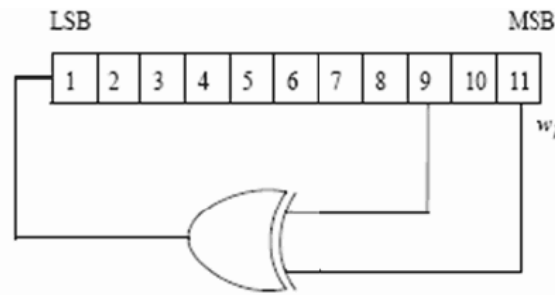
Fig. 2-16 PRBS generator for pilot modulation (from [2]).

following STC DL Zone IE() and 5 LSB of DL PermBase following AAS DL IE without Diversity Map support in the downlink. Five least significant bits of IDcell (as determined by the preamble) in the uplink. For downlink and uplink, b0 is MSB and b4 is LSB, respectively.

b5..b6 = set to the segment number + 1 as indicated by the frame preamble in the first downlink zone and in the downlink AAS zone with Diversity Map support, PRBS ID as indicated by the STC DL Zone IE or AAS DL IE without Diversity Map support in other downlink zone. 0b11 in the uplink. For downlink and uplink, b5 is MSB and b6 is LSB, respectively.

b7..b10 = 0b1111 (all ones) in the downlink and four LSB of the Frame Number in the uplink. For downlink and uplink, b7 is MSB and b10 is LSB, respectively.

Data Modulation

After the repetition block, the data bits are entered serially to the constellation mapper. Gray-mapped QPSK and 16-QAM shall be supported, whereas the support of 64-QAM is optional.

Pilot Modulation

In all permutations except uplink PUSC and downlink TUSC1, each pilot shall be transmitted with a boosting of 2.5 dB over the average non-boosted power of each data tone. The pilot

39

subcarriers shall be modulated according to

$$\Re\{c_k\} = \frac{8}{3}\left(\frac{1}{2} - w_k\right) \cdot p_k, \Im\{c_k\} = 0, \tag{2.26}$$

where p_k is the pilot's polarity for SDMA (spatial division multiple access) allocations in

AMC AAS zone, and $p = 1$ otherwise.

Preamble Pilot Modulation

The pilots in the downlink preamble shall be modulated according to

$$\Re\{PreambleP\ ilotModulation\} = 4 \cdot \sqrt{2} \cdot \left(\frac{1}{2} - w_k\right) \tag{2.27}$$

$$\Im\{PreambleP\ ilotModulation\} = 0. \tag{2.28}$$

2.7 Transmit Spectral Mask

Due to requirement of bandwidth-limited transmission, the transmitted spectral density of the

transmitted signal shall fall within the spectral mask as shown in Fig. 2-17 and Table 2-5 in

license-exempt bands. The measurements shall be made using 100 kHz resolution bandwidth

and a 30 kHz video bandwidth. The 0 dBr level is the maximum power allowed by the

relevant regulatory body. IEEE 802.16e dose not specify the power mask for the licensed

bands.

Table 2-5 Transmit Sprctral Mask for License-Exempt Bands

Bandwidth (MHz)	A	B	C	D
10	9.5	10.9	19.5	29.5
20	4.75	5.45	9.75	14.75
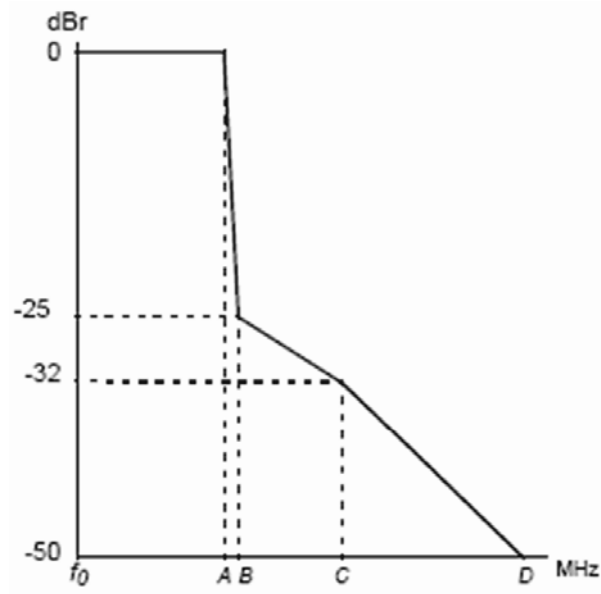
Fig. 2-17 Transmit spectral mask for license-exempt operation (from[4]).

2.8 Frequency and Timing Requirements

Timing Requirements

For any duplexing, all SSs shall acquire and adjust their timing such that all uplink OFDMA symbols arrive time coincident at the BS to an accuracy of ±25% of the minimum guard interval or better. For example, this translates into ±8 samples in the case of 1024-FFT OFDMA.

Frequency Requirements

At the BS, the transmitted center frequency, receive center frequency, and the symbol clock frequency shall be derived from the same reference oscillator. At the BS, the reference frequency accuracy shall be better than $\pm 2 \times 10^{-6}$.

At the SS, both the transmitted center frequency and the sampling frequency shall be derived from the same reference oscillator. Thereby, the SS uplink transmission shall be locked to the

BS, so that its center frequency shall deviate no more than 2% of the subcarrier spacing, compared to the BS center frequency.

During the synchronization period, the SS shall acquire frequency synchronization within the specified tolerance before attempting any uplink transmission. During normal operation, the SS shall track the frequency changes by estimating the downlink frequency offset and shall defer any transmission if synchronization is lost. To determine the transmit frequency, the SS shall accumulate the frequency offset corrections transmitted by the BS (for example in the RNG-RSP message), and may add to the accumulated offset an estimated UL frequency offset based on the downlink signal.

Chapter 3

Decision Directed Channel Estimation

This section describes some channel estimation schemes to deal with different environments. After finding the packet starting point, channel estimation is performed to recover the channel frequency response. In this Chapter, the channel estimation will be introduced in detail. Then, we give a brief overview of the relevant technique.

3.1 Channel Estimation Structure

The simple structure of the channel estimation is show as Fig. 3-1. The received signal is modeled as $Y(m) = H(m)X(m) + N(m)$, Y is the received signal, X is QPSK i.i.d. transmitted signal, H is with zero mean complex Gaussian distribution, N is white Gaussian noise, and m is subcarrier index.

$$\boxed{\text{Rx\_signal} \quad \text{Y}}$$

$$\downarrow$$

$$\boxed{\text{Initial Channel} \quad \tilde{\text{H}}}$$

$$\downarrow$$

$$\boxed{\begin{array}{c}\text{Iteration-}\\\text{Decision directed}\end{array}}$$

$$\downarrow$$
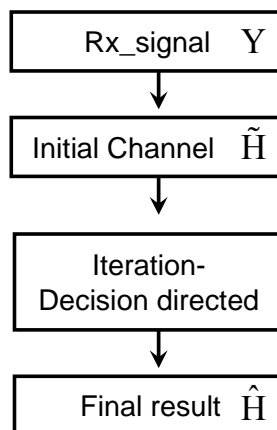
$$\boxed{\text{Final result} \quad \hat{\text{H}}}$$

Fig. 3-1 Channel estimation structure

There are two operations in the structure. One is the initial channel response estimation, the other is the iteration steps to refine the channel response until convergence.

3.2 Obtain The Initial Channel

We have some different choices to obtain the initial channel responses, namely, Pilot Symbol Aided, Linear Prediction, and Linear Interpolation.

■ Pilot Symbol Aided [17][18]

We add pilots $\tilde{\underline{X}}_{Np}$ to a symbol block. Denote N_p as the pilot numbers, and reasonably assume pilots $\tilde{\underline{X}}_{Np}$ are known. We can obtain the initial channel $\tilde{\underline{H}}_{Np}$, then put the initial channel $\tilde{\underline{H}}_{Np}$ into a low pass filter. The output of the low pass filter is the final result $\hat{\underline{H}}$.

■ Linear Prediction [15][16]

Suppose the last $p's$ symbol channels are known perfectly, we predict the $p+1$ channel from the previous $1 \sim p$ channels.

■ Linear Interpolation

We need a buffer to save a block of data. We use Pilot Symbol Aided in the first and last symbol to obtain channel, and the initial channels of the other symbols are obtained by the Linear Interpolation.

3.2.1 Pilot Symbol Aided

Channel estimators usually need some kind of pilot information as a point of reference. A
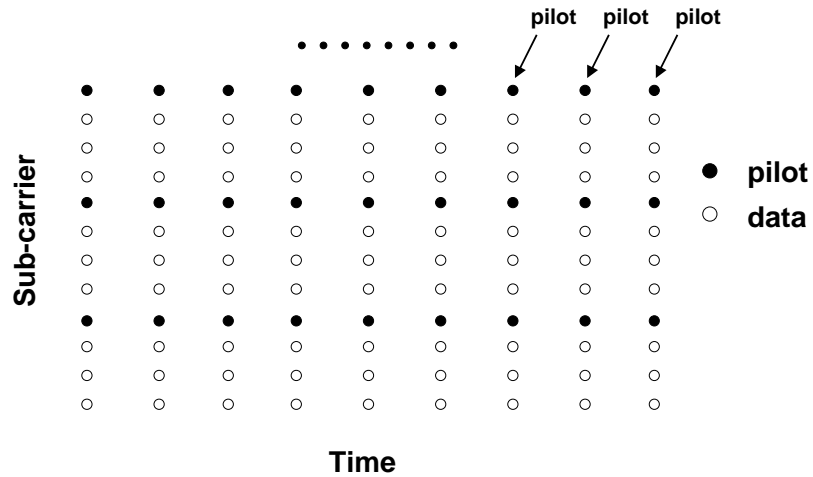
Fig. 3-2 Pilot Symbol Aided

fading channel requires constant tracking, so pilot information has to be transmitted more or less continuously. Decision-directed channel estimation can also be used. But even in these types of schemes, pilot information has to be transmitted regularly to mitigate error propagation. The structure of the Pilot Symbol Aided is show as the Fig. 3-2. The channel of every symbol was estimated by pilot. The initial channel estimation of every symbol was shown in the follow description,

$$\underline{\tilde{\mathbf{H}}}_{Np} = \begin{cases} [Y(m)/X(m)] \,, \ m = i(M/Np), 0 \leq i \leq Np-1 \\ [0] \qquad\qquad , \ \text{where } m \text{ is others} \end{cases} \tag{3.1}$$

The illustration is shown in Fig. 3-3
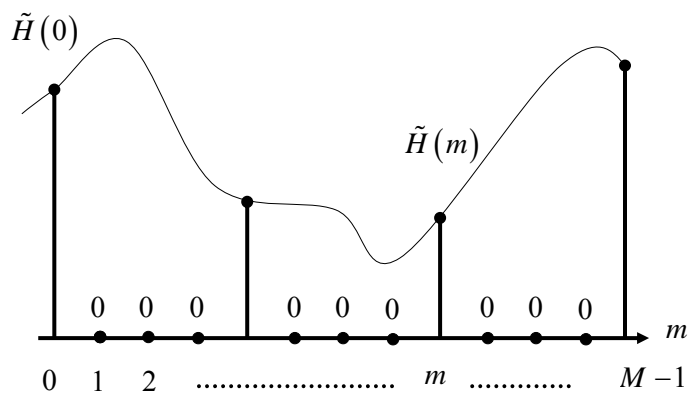
Fig. 3-3 Initial channel $\underline{\tilde{\mathbf{H}}}_{Np}$

$\mathbf{W}$ is the DFT matrix. N_p is the pilot numbers. The sub-carrier index m is in the pilot space.

Most of the energy in $\underline{\mathrm{h}}$ is contained in, or near, the first $(L+1)$, $\underline{\tilde{\mathrm{h}}}_{L+1} = \left[\tilde{h}_0, ..., \tilde{h}_{L+1} \right]^T$, the first $(L+1)$ taps of $\underline{\tilde{\mathrm{h}}}$.

$$\underline{\tilde{\mathrm{h}}}_{L+1} = \left(\left(\mathbf{W}_{N_\mathrm{p},(L+1)}^H \right) * \left(\mathbf{W}_{N_\mathrm{p},(L+1)} \right) \right)^{-1} \left(\mathbf{W}_{N_\mathrm{p},(L+1)}^H \right) \underline{\tilde{\mathrm{H}}}_{Np}$$

(3.2)

The complete channel estimation $\underline{\hat{\mathrm{H}}}$ of all the sub-carriers is computed from $\underline{\tilde{\mathrm{h}}}_{L+1}$ by

$$\underline{\tilde{\mathrm{H}}} = \mathbf{W}_{M,(L+1)} * \underline{\tilde{\mathrm{h}}}_{L+1}$$

(3.3)

whiere the DFT matrix $\mathbf{W}$ is

$$\mathbf{W}_{M,(L+1)} = \begin{bmatrix} 1 & 1 & \cdots & 1 \\ 1 & e^{-j2\pi\frac{1}{M}} & \cdots & e^{-j2\pi\frac{L-1}{M}} \\ \vdots & \vdots & \ddots & \vdots \\ 1 & e^{-j2\pi\frac{M-1}{M}} & \cdots & e^{-j2\pi\frac{L(M-1)}{M}} \end{bmatrix}_{M\times(L+1)}$$

(3.4)

The operations of the equations are the same as a low pass filter [23]. The equation is shown as Fig. 3-4 Low pass filter
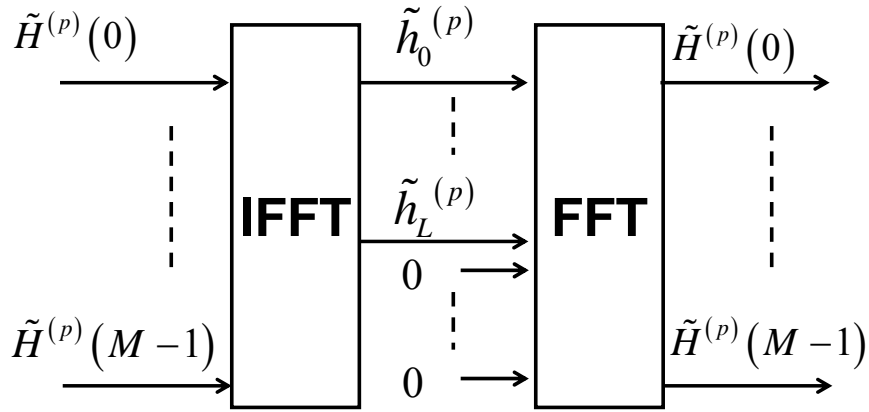
Fig. 3-4 Low pass filter

The parameter N_p has large correlation with the length of the channel impulse response L and cyclic prefix length N_{cp}. Now, we discuss the relationship of the pilot number N_p, the channel length L, and the cyclic prefix length N_{cp}. If the real channel impulse response and channel frequency response are shown as Fig. 3-5 and Fig. 3-6
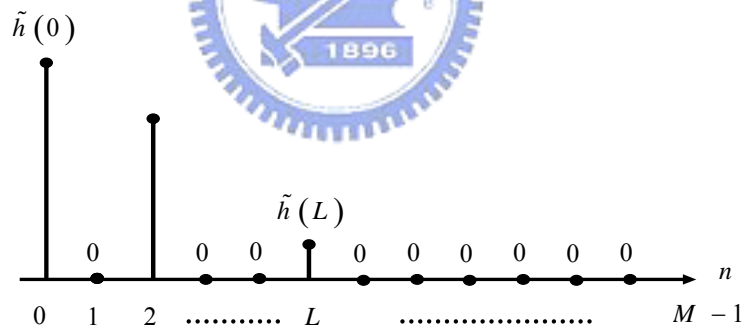
Fig. 3-5 Real channel impulse response
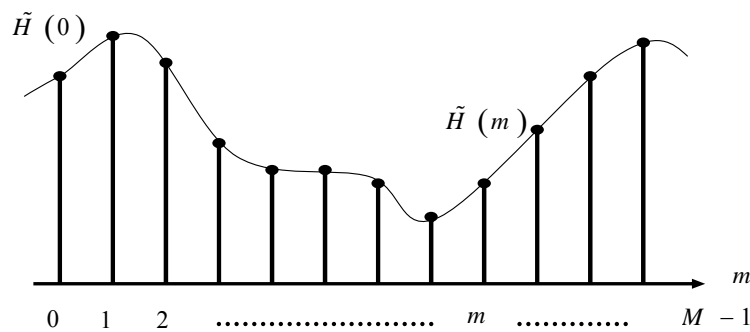
Fig. 3-6 Real channel frequency response
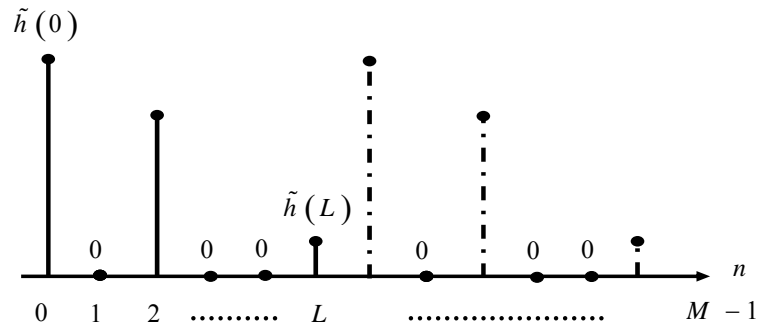
Fig. 3-7 Initial channel impulse response $\underline{\tilde{\mathbf{h}}}_{Np}$
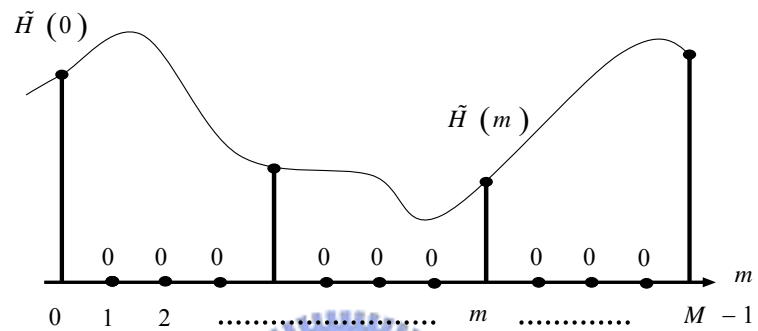
Fig. 3-8 Initial channel frequency response $\underline{\tilde{\mathbf{H}}}_{Np}$

In OFDM system, we assume the channel impulse responses are time invariant during a symbol time, and the cyclic prefix length N_{cp} is always larger than channel impulse response length L. Because we want to reduce the inter-symbol interference (ISI) perfectly, so, the cyclic prefix length N_{cp} is larger than the channel length L always. Than we just discuss the relationship between N_{cp} and N_{p} during a symbol time.

■ $N_{cp} \le N_{p}$

According to the sampling theory, the relationship between channel impulse response and channel frequency response can be shown in Fig. 3-7 and Fig. 3-8. According to the figures, we know that the initial channel $\underline{\tilde{\mathbf{H}}}_{Np}$ through to the low pass filter still close to the

48

real channel impulse response.

■ $N_p < N_{cp}$

Similarly, the relationship between channel impulse response and channel frequency response are shown as Fig. 3-9 and Fig. 3-10.

We know that, if sampling rate is smaller than Nyquist frequency in frequency domain, the aliasing will happen, in the time domain.

According to Fig. 3-9 and Fig. 3-10, we know that the initial channel $\underline{\tilde{H}}_{Np}$ through to the low pass filter not close to the real channel. Because there will be aliasing on impulse
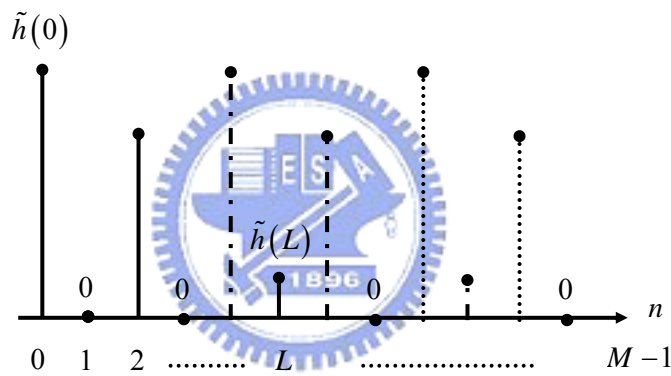
Fig. 3-9 Initial channel impulse response $\underline{\tilde{h}}_{Np}$
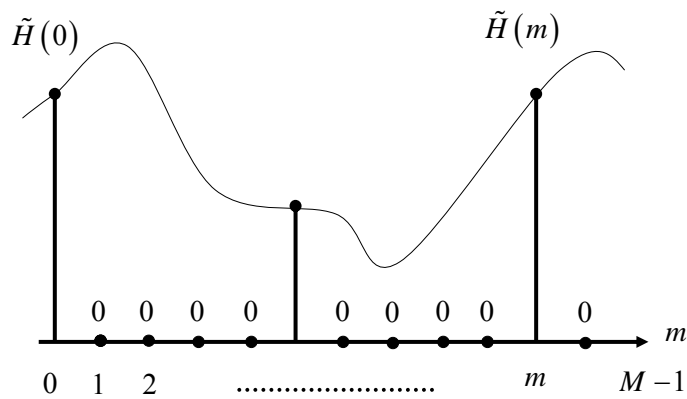
Fig. 3-10 Initial channel frequency response $\underline{\tilde{H}}_{Np}$

49
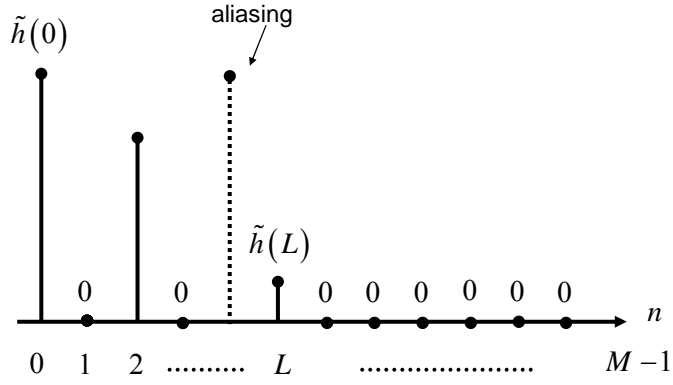
Fig. 3-11 Final resource of the channel impulse response.

response. According to the discussion, the parameter pilot number Np must be large than N_{cp} or equal to N_{cp}.

3.2.2 Linear Prediction

In this section, we introduce autoregressive (AR) model. When the p th-order AR ($\text{AR}(p)$) hypermodel for the frequency-selective fading channel is employed, we obtain a linear dynamic system which can be described by the following state-space model, the structure of the Pilot Symbol Aided is show as the Fig. 3-12

$$h_{l,t} = \left(\sum_{i=1}^{p} a_{l,i} h_{l,t-i} \right) + w_{l,t} \quad , \quad 0 \le l \le L$$

(3.5)

Specifically, the channel process $h_{l,t}$ is defined as a channel impulse at t symbol and l th path, $a_{l,i}$ is defined as weight numbers of p th-order channel $h_{l,t-1}, h_{l,t-2}, h_{l,t-3}, ..., h_{l,t-p}$.
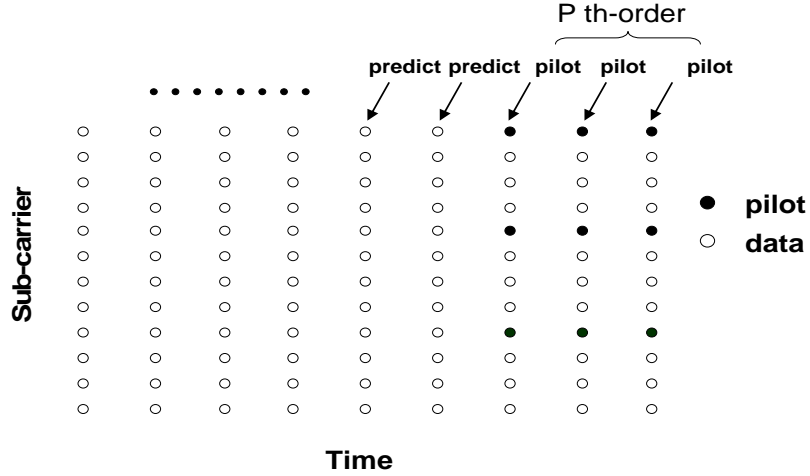
Fig. 3-12 Linear Prediction

is the Gaussian process noise, and it is assumed to be circular and independent of the receiver

noise n. Because multi-path are independent and uncorrelated, so the weight numbers $a_{l,i}$

are calculated separately. We want to predict the tth symbol channel the from pth-order

channel $h_{l,t-1}, h_{l,t-2}, h_{l,t-3}, ..., h_{l,t-p}$ as

$$h_{l,t} = \left(\sum_{i=1}^{p} a_{l,i} h_{l,t-i} \right) + w_{l,t} \quad , \quad 0 \le l \le L$$

$$\tilde{h}_{l,t} = \left(\sum_{i=1}^{p} a_{l,i} h_{l,t-i} \right) \quad , \quad 0 \le l \le L \tag{3.6}$$

To find the coefficient $a_{l,1}, a_{l,2}, a_{l,3}, ..., a_{l,p}$ so as to minimize the index of performance J

$$J = \mathrm{E}\left[w_{l,t}^{2} \right], \text{ where } w_{l,t} = h_{l,t} - \tilde{h}_{l,t} \tag{3.7}$$

Let $\{h_{l,t}\}$ be stationary with autocorrelation function $R_h(\tau)$

$$J = \mathrm{E}\left[\left(h_{l,t} - \sum_{\tau=1}^{p} a_{l,\tau} h_{l,t-\tau}\right)^2\right]$$

$$= \mathrm{E}\left[h^2_{l,t}\right] - 2\sum_{\tau=1}^{p} a_{l,\tau}\, \mathrm{E}\left[h_{l,t} h_{l,t-\tau}\right] + \sum_{\tau=1}^{p}\sum_{j=1}^{p} a_{l,\tau} a_{l,j}\, \mathrm{E}\left[h_{l,t-\tau} h_{l,t-j}\right]$$

$$= R_h(0) - 2\sum_{\tau=1}^{p} a_{l,\tau} R_h(\tau) + \left(2\sum_{\tau=1}^{p}\sum_{j>\tau}^{p} a_{l,\tau} a_{l,j} R_h(\tau - j) + \sum_{\tau=1}^{p} a^2_{l,\tau} R_h(0)\right)$$

$$\frac{\partial}{\partial h_{l,i}} J = -2R_h(i) + \left(2\sum_{j=i+1}^{p} a_{l,j} R_h(i-j) + 2\sum_{\tau=1}^{i-1} a_{l,\tau} R_h(\tau - i) + 2a_{l,i} R_h(0)\right)$$

$$= -2R_h(i) + 2\sum_{j=1}^{p} a_{l,j} R_h(i-j) = 0$$

(3.8)

$$\sum_{j=1}^{p} a_{l,j} R_h(i-j) = R_h(i) \text{ for } 1 \leq i \leq p$$

(3.9)

The above optimality equations are called the Wiener-Hopf equations for linear prediction. It can be rewritten in matrix form as

$$\begin{bmatrix} R_h[0] & R_h[1] & \cdots & R_h[p-1] \\ R_h[1] & R_h[0] & \cdots & R_h[p-2] \\ \vdots & \vdots & \ddots & \vdots \\ R_h[p-1] & R_h[p-2] & \cdots & R_h[0] \end{bmatrix}\begin{bmatrix} a_{l,1} \\ a_{l,2} \\ \vdots \\ a_{l,p} \end{bmatrix} = \begin{bmatrix} R_h[1] \\ R_h[2] \\ \vdots \\ R_h[p] \end{bmatrix}$$

(3.10)

Optimal solution is given by

$$\begin{bmatrix} a_{l,1} \\ a_{l,2} \\ \vdots \\ a_{l,p} \end{bmatrix} = \begin{bmatrix} R_h[0] & R_h[1] & \cdots & R_h[p-1] \\ R_h[1] & R_h[0] & \cdots & R_h[p-2] \\ \vdots & \vdots & \ddots & \vdots \\ R_h[p-1] & R_h[p-2] & \cdots & R_h[0] \end{bmatrix}^{-1}\begin{bmatrix} R_h[1] \\ R_h[2] \\ \vdots \\ R_h[p] \end{bmatrix}$$

(3.11)

- Toeplitz (square) matrix

Any square matrix of the form

$$
\begin{bmatrix}
a_0 & a_1 & \cdots & a_{p-1} \\
a_1 & a_0 & \cdots & a_{p-2} \\
\vdots & \vdots & \ddots & \vdots \\
a_{p-1} & a_{p-2} & \cdots & a_0
\end{bmatrix}_{p \times p}
\tag{3.12}
$$

Is said to be Toeplitz.

3.2.3 Linear Interpolation

If we have B symbols in an OFDM block, we use Pilot Symbol Aided in first symbol of the block, and obtain this symbol channel. Than, we need a buffer to save a block data, and the first symbol of the next block. The initial channels of the other symbols are obtained by the Linear Interpolation. The structure is shown as Fig. 3-13

The first channel of the block1 is $\hat{\underline{H}}(t_0)$, the first channel of the block2 is $\hat{\underline{H}}(t_1)$. We save the block1 datas and $\hat{\underline{H}}(t_1)$ to the buffer, the other initial channel
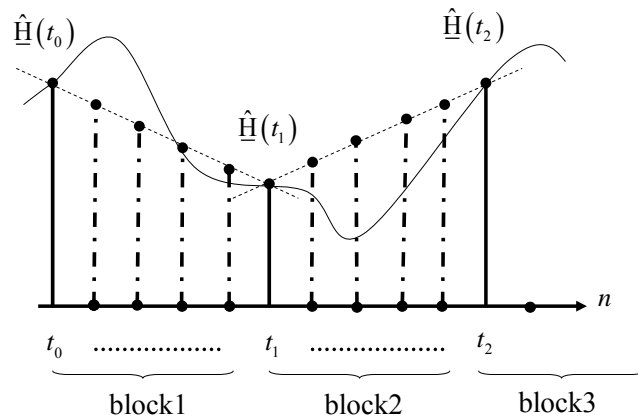
Fig. 3-13 Linear Interpolation

53

$$\left[\tilde{\underline{H}}(t_0+1), \tilde{\underline{H}}(t_0+2), ..., \tilde{\underline{H}}(t_0+B-1) \right] \text{ between } \hat{\underline{H}}(t_0) \text{ and } \hat{\underline{H}}(t_1) \text{ are shown as}$$

$$\hat{\underline{H}}(t_0+b) = \hat{\underline{H}}(t_0) + \frac{\hat{\underline{H}}(t_1) - \hat{\underline{H}}(t_0)}{B} b \ , \ 0 \le b \le B-1 \qquad (3.13)$$

After the last action, the initial channel is obtained. If the OFDM system active without the iteration step, just take the initial channel as a final result, the result is not close to the real channel. If the initial channel is obtained by Pilot Symbol Aided, the final result is not very terrible. But if the linear prediction is used, the error between initial channel and real channel will be accumulating to next initial channel. So, we do some iteration to close the real channel.

We have two difference choice to use. One is Decision directed, the other is Expectation Maximization (EM) Algorithm.

3.3 Iteration- Decision Directed

The iteration processing was introduced as follows. Before doing the iteration, the input of the lowpass filter is called the initial channel estimation $\tilde{\underline{H}}^{(0)}$, but after the iterative is used, the output of the lowpass filter is the pth iterativel result $\hat{\underline{H}}^{(p)}$. The iteration process is shown in the Fig. 3-14. The initial channel estimation $\tilde{\underline{H}}^{(0)}$ is the input of the iteration processing, pass by lowpass filter, some of the AWGN is reduced. The receiver signal $\underline{Y}$ and the output of the lowpass filter $\hat{\underline{H}}^{(0)}$ are used to calculate the detection signal $\hat{\underline{X}}^{(0)}$. The detection signal $\hat{\underline{X}}^{(0)}$ are used to be new pilots. After p times iteration, the output of the LPF $\hat{\underline{H}}^{(p+1)}$ is the final channel. The next iterative result of the detection signal is $\hat{\underline{X}}^{(p+1)}$.

$\tilde{\underline{H}}^{(p)}$ → LPF → $\hat{\underline{H}}^{(p)}$ → Quantize $\dfrac{Y(m)}{\hat{H}^{(p)}(m)}$ → $\hat{\underline{X}}^{(p)}$ → $Y \times \hat{X}^{H}$ → $\tilde{\underline{H}}^{(p+1)}$
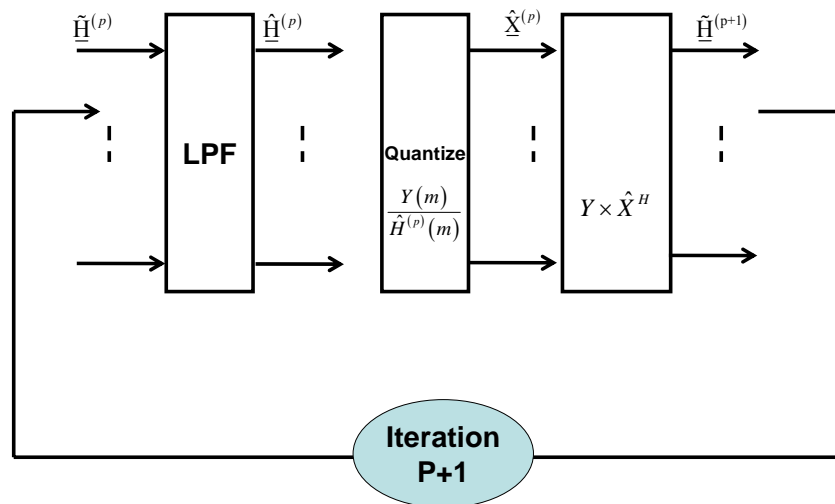
Iteration
P+1

Fig. 3-14 Decision directed iteration process

The iteration stop until the channel estimation $\hat{\underline{H}}^{(p+1)}$ is stable.

3.4 Decision Directed Channel Estimator

Base on the last discussion, we have three methods to obtain the initial channel, and two

iteration methods.

■ Initial channel

1. Pilot Symbol Aided

2. Linear Prediction

3. Linear Interpolation

■ Iteration- Decision directed

We combine the methods to be six channel estimators

1. Decision directed Pilot Symbol Aided (DD Pilot)

2. Decision directed Linear Prediction (DD AR)

3. Decision directed Linear Interpolation (DD LI)

3.5 Channel System Environment

In this section, we first show the simulation environment for our study, including the system parameters and channel environments.

3.5.1 System Parameters

We have to specify the system parameters from all usable values provided by 802.16e so that the simulation environment could be constructed. The standard is very flexible in choice of bandwidth and cyclic prefix length. However, it would be difficult to conduct the simulation and implementation study without some particular sets of parameters. Hence we pick some sets of parameters shown in this section. The system profile we select is Wireless random generated binary data. The frame duration could be 5, or 10ms. Other parameter values are

Table 3-1 System Parameters Used in Our Study

Parameters	Values		
System Channel Bandwidth (MHz)	10	10	20
Sampling Frequency (MHz)	11.2	11.2	22.4
FFT Size	1024	2048	2048
Sub-carrier Spacing (kHz)	10.94	5.47	10.94
Useful Symbol Time (μsec)	91.4	182.8	91.4
Guard Time (μsec)	11.4	22.8	11.4
OFDM Symbol Time (μsec)	102.9	205.7	102.9

in Table 3-1

3.5.2 Channel Environments

Typical models of the wireless communication channel include additive noise and multi-path fading. For channel simulation, noise and multipath fading are described as random processes, so they can be algorithmically generated as well as mathematically analyzed.

3.5.2.1 Gaussian Noise

The simplest kind of channel is the additive white Gaussian noise (AWGN) channel, where the received signal is only subject to added noise. A major source of this noise is the thermal noise in the amplifiers which may be modeled as Gaussian with zero mean and constant variance. Incomputer simulations, random number generators may be used to generate Gaussian noise of given power to obtain a particular signal-to-noise ratio (SNR).

Table 3-2 Terrain Type vs. SUI Channels

Terrain Type	SUI Channels
A: hilly terrain, heavy tree	SUI-5, SUI-6
B: between A and C	SUI-3, SUI-4
C: flat terrain, light tree	SUI-1, SUI-2

Table 3-3 General characteristics of SUI channels

Doppler	Low delay spread	Moderate delay spread	High delay spread
Low	SUI-1, SUI-2, SUI3		SUI-5
High		SUI-4	SUI-6

3.5.2.2 Slow Fading Channel

In slow fading, multipath propagation may exist, but the channel coefficients do not change significantly over a relatively long transmission period. The channel impulse response over a short time period can be modeled as

$$h(\tau) = \sum_{l=0}^{L-1} \alpha_l e^{j\theta_l} \delta(\tau - \tau_l).$$

where L is the number of multipaths, α_l and τ_l are respectively the amplitude and the delay of the lth multipath, and θ_l represents the phase shift associated with path l. These parameters are time-invariant in a short enough time period.

3.5.2.3 Fast Fading Channel

With sufficiently fast motion of either the transmitter or the receiver, the coefficient of each propagation path becomes time varying. The equivalent baseband channel impulse response can then be better modeled as

$$h(\tau, t) = \sum_{l=0}^{L-1} \alpha_l(t) e^{j\theta_l(t)} \delta(\tau - \tau_l).$$

Note that α_l and θ_l are now functions of time. But τ_l is still time-invariant, because the path delays usually change at a much slower pace than the path coefficients. The channel coefficients are often modeled as complex independent stochastic processes. If there is no line-of-sight (LOS) path between the transmitter and the receiver, each path may be made of the superposition of many reflected paths, yielding a Rayleigh fading characteristic. A commonly used method to simulate Rayleigh fading is Jakes' fading model, which is a deterministic method for simulating time-correlated Rayleigh fading waveforms.

Table 3-4 SUI-1 Channel Model

	Relative delay (μs or sample number)		Average power	
Tap	(μs)	(normal)	(dB)	(normalized)
1	0	0	0	0.9610
2	0.4	4	-15	0.0303
3	0.9	10	-20	0.0096

Table 3-5 SUI-2 Channel Model

	Relative delay (μs or sample number)		Average power	
Tap	(μs)	(normal)	(dB)	(normalized)
1	0	0	0	0.9135
2	0.4	4	-12	0.0576
3	1.1	12	-15	0.0289

Table 3-6 SUI-3 Channel Model

	Relative delay (μs or sample number)		Average power	
Tap	(μs)	(normal)	(dB)	(normalized)
1	0	0	0	0.7061
2	0.4	4	-5	0.2233
3	0.9	10	-10	0.0706

Table 3-7 SUI-4 Channel Model

	Relative delay (μs or sample number)		Average power	
Tap	(μs)	(normal)	(dB)	(normalized)
1	0	0	0	0.6424
2	1.5	4	-4	0.2557
3	4	16	-8	0.1018

Table 3-8 SUI-5 Channel Model

	Relative delay (μs or sample number)		Average power	
Tap	(μs)	(normal)	(dB)	(normalized)
1	0	0	0	0.7061
2	4	45	-5	0.2233
3	10	112	-10	0.0706

Table 3-9 SUI-6 Channel Model

	Relative delay (μs or sample number)		Average power	
Tap	(μs)	(normal)	(dB)	(normalized)
1	0	0	0	0.8773
2	14	156	-10	0.0877
3	20	224	-14	0.0349

Table 3-10 ETSI "Vehicular A" Channel Model in Different Units

	Relative delay (μs or sample number)		Average power	
Tap	(μs)	(normal)	(dB)	(normalized)
1	0	0	0	0.4850
2	0.31	3	-1	0.3852
3	0.71	8	-9	0.061
4	1.09	12	-10	0.0485
5	1.73	19	-15	0.0153
6	2.51	28	-20	0.0049

3.5.2.4 Power-Delay Profile Model

For simplicity in analysis and simulation, the delay τ_l in the above two models can be

discretized to have a certain easily manageable granularity. This results in a tapped-delay-line

model for the channel impulse response, where the spacing between any two taps is an integer

multiple of the chosen granularity. For convenience, one may excise the initial delay and

make $\tau_0 = 0$. Often, it is convenient to normalize the path powers relative to the strongest path. And, often, the first path has the highest average power.

The channel model used here is a modification of the Stanford University Interim (SUI) channel models propsed in [19]. These models, for a collect of scenarios, provide the parameters to model the various random phenomena involved with a simulation; of course there are many possible combinations of these parameters to obtain such channel descriptions.

A set of 6 typical channels was selected for the three most common terrain categories that are typical of the continental United States. The parametric view of the SUI channels is summarized in Table 3-2 and Table 3-3

Scenario for SUI channels

- Cell size: 7km

- Base station antenna height: 30 m

- Receiver antenna height: 6 m

- Base station antenna beamwidth: 120°

- Receiver antenna beamwidth: omnidirectional $\left(360°\right)$ and 30°

- Vertical polarization only

We list all of the SUI channel models in Table 3-4 to Table 3-9 that will be used in our simulations below.

Another channel model chosen from one of the channel environments defined by ETSI is used in this thesis. The model is as shown in Table 3-10. This is a channel model for the vehicular test environment, which the tested speed is from 120 km/h to 500 km/h. This

environment is characterized by larger cells and higher transmit power, and is valid for NLOS case only and describes worse case propagation. Channel A is the low delay spread case that occurs frequently. See [20] for more details.
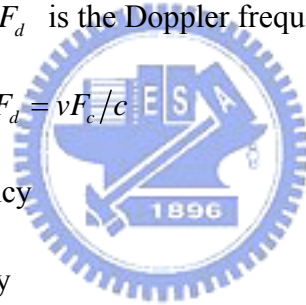
3.6 Simulation

We show the simulation result as in Fig. 3-15~Fig. 3-20 , there are four cases to be discussing,

■ SUI3 for $v = 100$ km/hr, $v = 240$ km/hr

■ SUI5 for $v = 100$ km/hr, $v = 240$ km/hr

■ Vehicular A for $v = 100$ km/hr, $v = 240$ km/hr

Ts is the sampling time, and F_d is the Doppler frequency, where

$$F_d = vF_c/c$$

■ F_d Doppler frequency

■ F_c carrier frequency

■ v velocity of mobile

■ c velocity of light

This simulation are base on SUI-3 channel, SUI-5 channel and Vehicular A. The subcarrier number M is 1024, cyclic prefix length $N_{cp} = M/8$. Carrier frequency $F_c = 3.5$ GHz. Bandwidth $BW = 11.2$ MHz, block length $B = 4$ symbols in Linear Interpolation. When Linear Interpolation is used, block length B should not too large, the symbol channels of this block are still linear, so the Linear Interpolation can work. If B is too large, the channels are not linear, so the Linear Interpolation can not work effective.
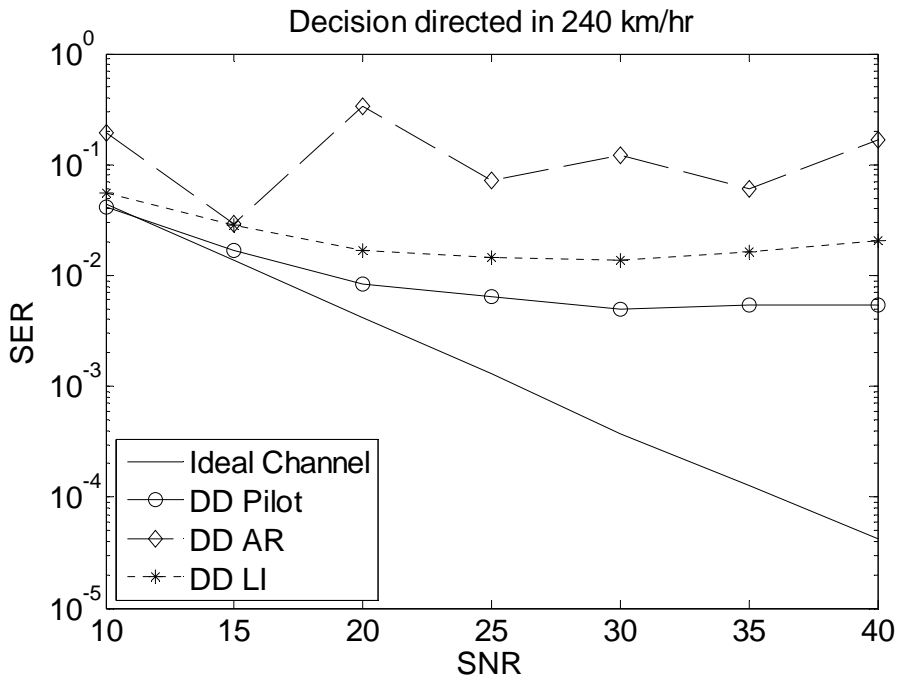
3.6.1 SUI3

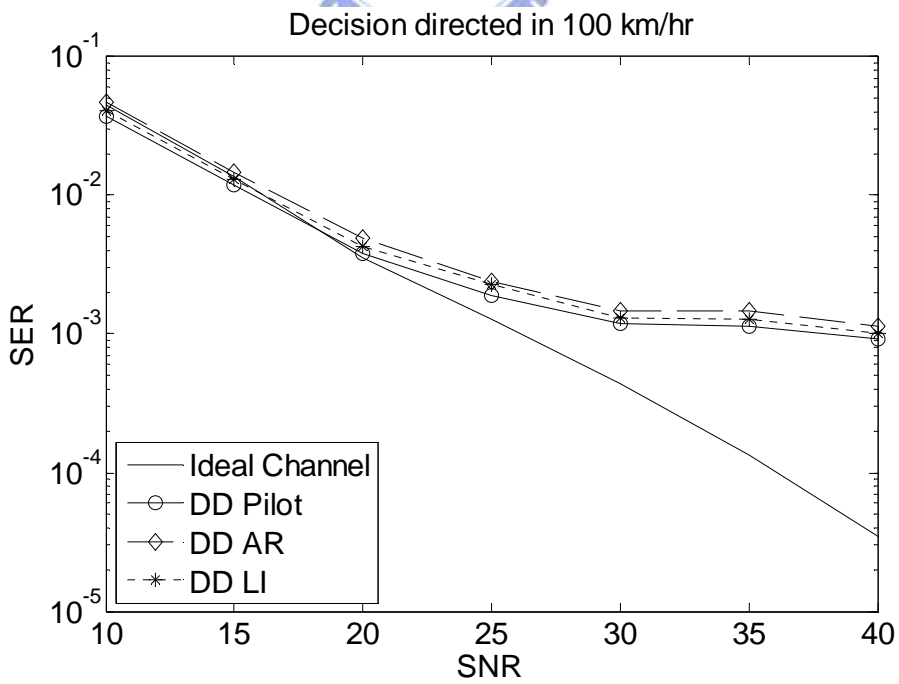**Fig. 3-15** SER performance for DD in 240 km/hr

Fig. 3-16 SER performance for DD in 100 km/hr

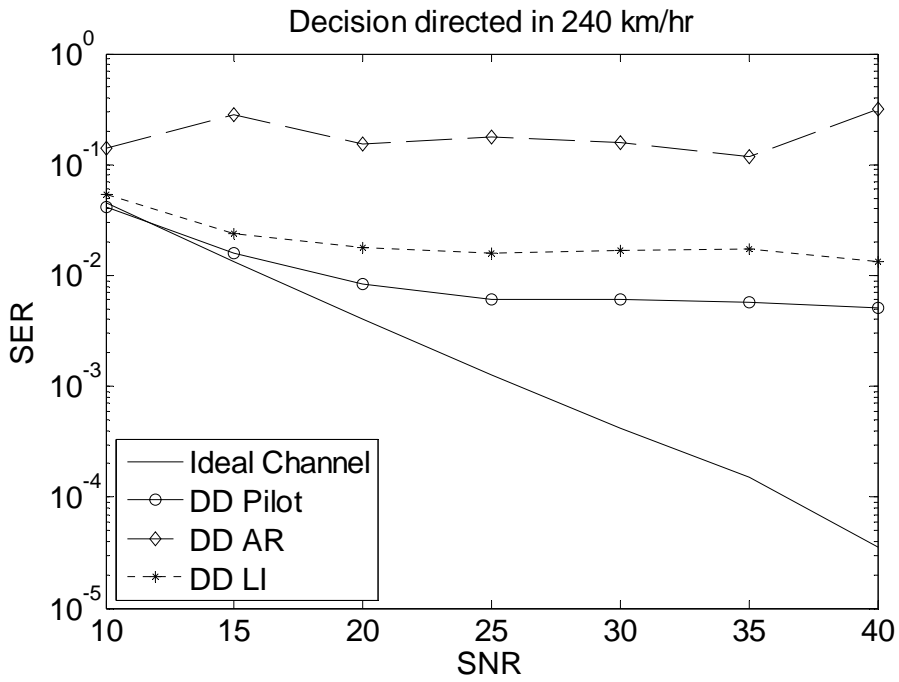## 3.6.2 SUI5

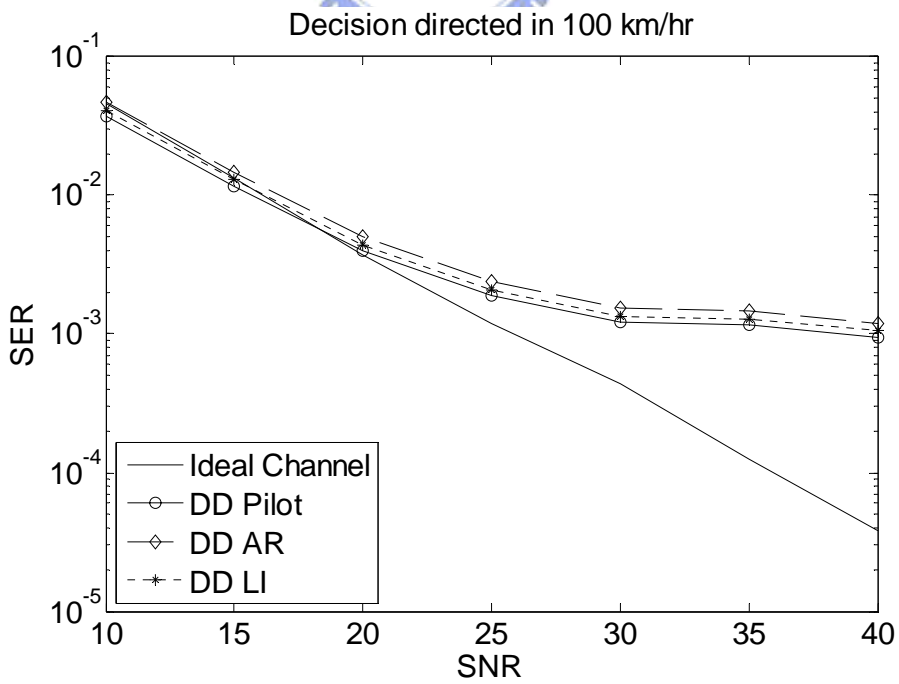**Fig. 3-17** SER performance for DD in 240 km/hr

Fig. 3-18 SER performance for DD in 100 km/hr

3.6.3 Vehicular A
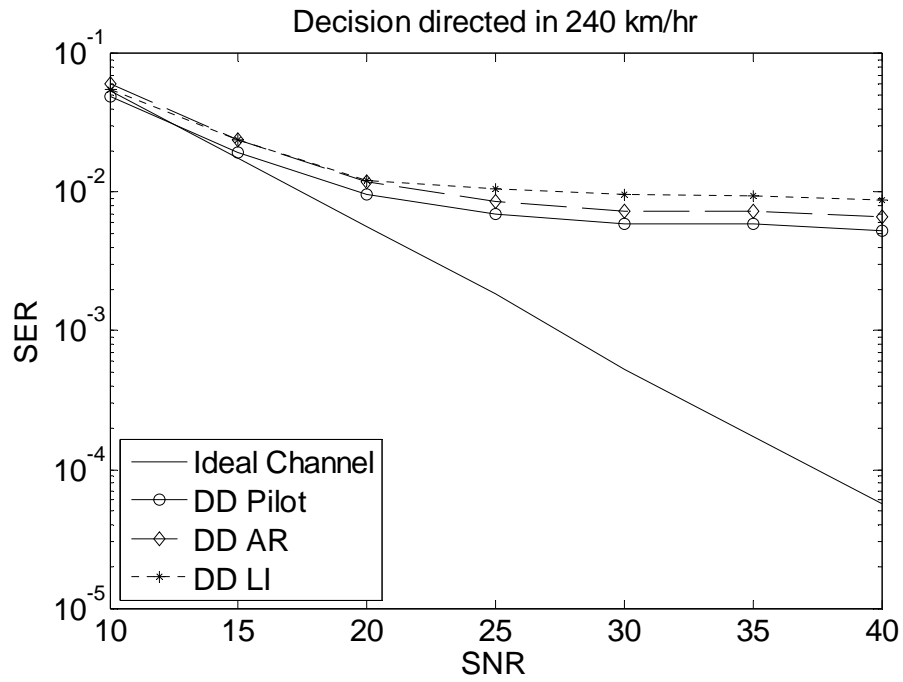
Fig. 3-19 SER performance for DD in 240 km/hr
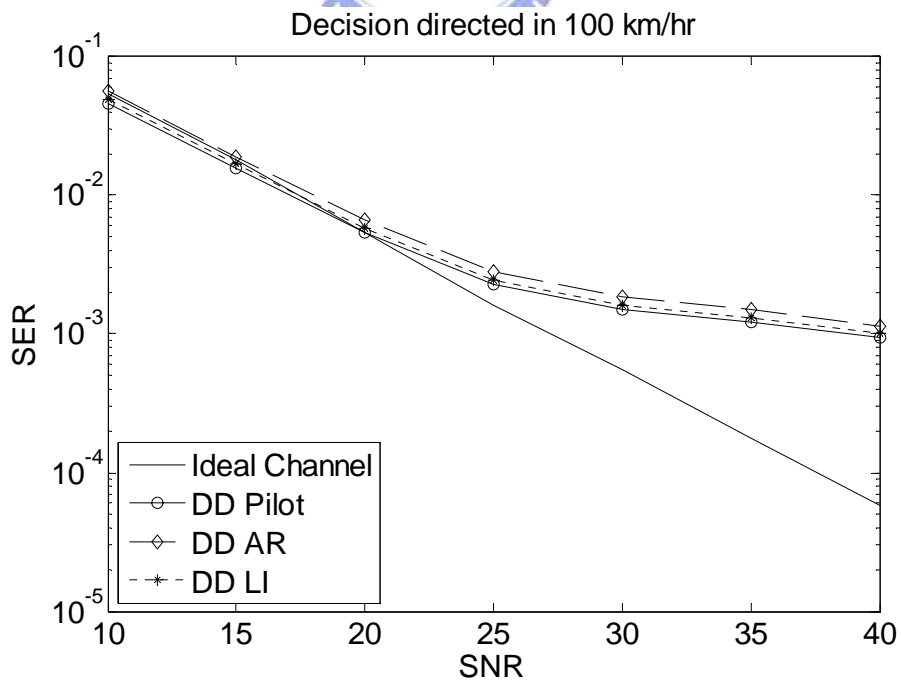
Fig. 3-20 SER performance for DD in 100 km/hr

According to the simulations, we can see that the Decision directed-AR estiamtor can not work in high speed for SUI-3 and SUI-5. The Decision directed-Pilot Symbol Aided has the best performance of the symbol error rate (SER), but it has the highest pilot number. The Decision directed-Linear Interpolation can work in each environments, but it need to use one block data to estimate channel.

Chapter 4

Expectation Maximization

Channel Estimation

4.1 Introduction of Expectation Maximization (EM) [16]

The EM algorithm [28, [29] is a technique for finding maximum likelihood (ML) estimates of

system parameters in a broad range of problems where observed data are incomplete. The EM

algorithm consists of two iterative steps: the expectation (E) step and the maximization (M)

step. The E-step is performed with respect to the unknown underlying parameters, using

current estimates of the parameters, conditioned upon the incomplete observations.

TheM-step then provides new estimates of the parameters that maximize the expectation of

the log-likelihood function defined over complete data, conditioned on the most recent

observation and the last estimate. These two steps are iterated until the estimated values

converge.

The EM algorithm [28], [29] is an iterative method to find the ML estimates of parameters in

the presence of unobserved data. The idea behind the algorithm is to augment the observed

data with latent data, which can be eithermissing data or parameter values, so that the

likelihood function conditioned on the data and the latent data has a form that is easy to

manipulate. The algorithm can be broken down into two steps: the E-step and the M-step. We

assume that the data Z ("complete" data) can be separated into two components,

$Z = (X, Y)$, where Y are the observed data ("incomplete" data) and X are the missing data. We denote θ as the unknown parameter we try to estimate from X.

The E-step finds $Q(\theta | \theta^{(p)})$, the expected value of the log-likelihood of θ, $\log f(Z | \theta)$, where the expectation is taken with respect to X conditioned on Y and the latest estimate of θ, $\theta^{(p)}$

$$Q(\theta | \theta^{(p)}) = E\left\{\log f(Z | \theta) | Y, \theta^{(p)}\right\}.$$

The M-step then finds $\theta^{(p+1)}$, the value of θ that maximizes $Q(\theta | \theta^{(p)})$ over all possible values of θ:

$$\theta^{(p+1)} = \arg \max_{\theta} Q(\theta | \theta^{(p)})$$

This procedure is repeated until the sequence $\theta^{(0)}$, $\theta^{(1)}$, $\theta^{(2)}$,…converges. The EM algorithm is constructed in such a way that the sequence of $\theta^{(p)}$'s converges to the ML estimate of θ.

Under our system model:

$$Y(m) = H(m) X(m) + N(m)$$

Z is   "unobserved data" or "complete data".

Y is   "observed data" or "incomplete data".

H is unknown parameter we try to estimates.

X is   "latent data" or "missing data".

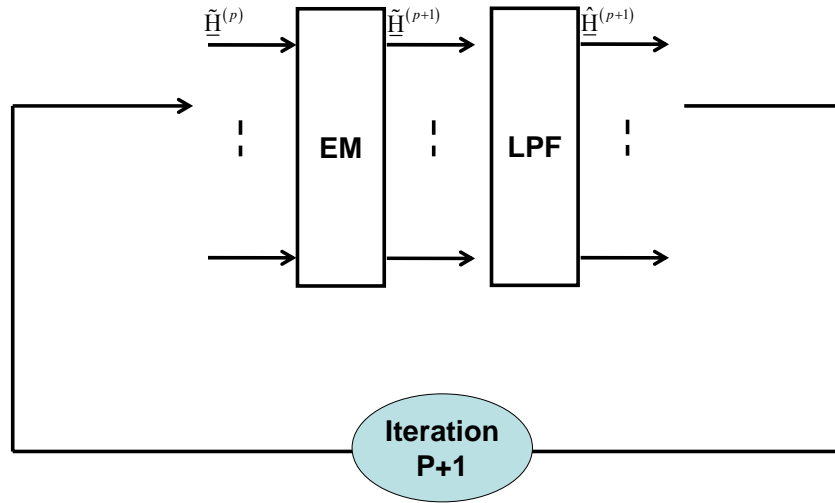## 4.2 Iteration- Expectation Maximization (EM)
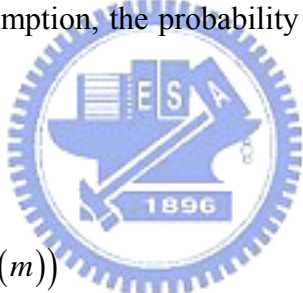
Fig. 4-1 EM Algorithm iteration process

Due to the Gaussian noise assumption, the probability density function of Y given X and

H is given by

$$
f\left(Y(m) \mid X(m), H(m)\right)
$$
$$
= \frac{1}{\sqrt{2\pi\sigma_n^2}} \exp\left\{-\frac{1}{2\sigma_n^2} \mid Y(m) - H(m) X(m) \mid^2 \right\}. \tag{4.1}
$$

By assuming that all C symbols are equally likely and averaging the condition pdf over the

variable X, we obtain the pdf of Y given H as follows

$$
f\left(Y(m) \mid H(m)\right)
$$
$$
= \sum_{i=1}^{C} \frac{1}{C\sqrt{2\pi\sigma_n^2}} \exp\left\{-\frac{1}{2\sigma_n^2} \mid Y(m) - H(m) X_i \mid^2 \right\}. \tag{4.2}
$$

70

We assume that the frequency-domain signal X of a given sub-carrier represents a QPSK signal with constellation size C (=4).

$$X_i = e^{j\left[\frac{\pi}{4}(2i-1)\right]} \quad i = 1, 2, 3, 4$$

Each iterative process $p = 0, 1, 2, ...$ in the EM algorithm for estimating H from Y consists of the following two steps

E-step

$$
\begin{aligned}
&Q\left(H(m) \mid H^{(p)}(m)\right) \\
&= E_X \left\{ \log f\left(Y(m), X(m) \mid H(m)\right) \mid Y(m), H^{(p)}(m)\right\};
\end{aligned}
\tag{4.3}
$$

M-step

$$\tilde{H}^{(p+1)}(m) = \arg\max_H Q\left(H(m) \mid H^{(p)}(m)\right), \tag{4.4}$$

$$
\begin{aligned}
&Q\left(H \mid H^{(p)}\right) \\
&= \sum_{i=1}^{C} \log\left\{\frac{1}{C} f\left(Y(m) \mid H(m), X_i\right)\right\} \frac{f\left(Y(m) \mid H^{(p)}(m), X_i\right)}{Cf\left(Y(m) \mid H^{(p)}(m)\right)}.
\end{aligned}
\tag{4.5}
$$

Before doing Expectation Maximization (EM) Algorithm, the initial channel estimation $\tilde{\underline{H}}^{(0)}$ is the input of the EM step, the output of the EM Algorithm $\tilde{\underline{H}}^{(1)}$ is shown as

71

$$\tilde{H}^{(1)}(m) = Y(m)\left\{\sum_{i=1}^{4} w_i^{(0)}(X_i)^*\right\}, \quad 0 \le m \le M-1 \tag{4.6}$$

w_i is the weighing of the signal X_i. In QPSK, $X_i = e^{j\left[\frac{\pi}{4}(2i-1)\right]}$ $i = 1, 2, 3, 4$. The weighing w_i is shown as

$$w_i^{(0)} = \frac{\exp^{\frac{-\left|Y(m)-\tilde{H}^{(0)}(m)X_i\right|^2}{2\sigma_n^2}}}{\sum_{i=1}^{4} \exp^{\frac{-\left|Y(m)-\tilde{H}^{(0)}(m)X_i\right|^2}{2\sigma_n^2}}}, \quad 1 \le i \le 4 \tag{4.7}$$

Than the EM channel estimation $\tilde{\underline{H}}^{(1)}$ is passed LPF to reduce noise. The output of the LPF is $\hat{\underline{H}}^{(1)}$. After p times iteration, the output of the LPF $\hat{\underline{H}}^{(p+1)}$ is the final channel. The final result of the detection signal is $\hat{\underline{X}}^{(p+1)}$. The iteration stop until the channel estimation $\hat{\underline{H}}^{(p+1)}$ is stable. The final result $\hat{\underline{H}}^{(p+1)}$ is shown as

$$\tilde{H}^{(p+1)}(m) = Y(m)\left\{\sum_{i=1}^{4} w_i^{(p)}(X_i)^*\right\}, \quad 0 \le m \le M-1 \tag{4.8}$$

4.3 Estimate Noise Power

Base on the Expectation Maximization (EM) Algorithm, we know that the noise power σ_n^2 is necessary. We can obtain the parameter easily. When we received one symbol signal, the receiver signal are shown as

$$Y(m) = H(m)X(m) + N(m) \tag{4.9}$$

We can obtain the noise power as

$$
\begin{aligned}
&E\{Y^H Y\} \\
&= E\{(HX+N)^H (HX+N)\} \\
&= E\{(HX)^H (HX)\} + 0 + E\{N^H N\} \\
&= E\{H^H (X^H X)H\} + \sigma_n^2 \\
&= E\{H^H H\} + \sigma_n^2 \\
&= \sigma_H^2 + \sigma_n^2 \\
&= 1 + \sigma_n^2
\end{aligned}
\tag{4.10}
$$

We assume the channel gain was normalize to 1, the noise power σ_n^2 is shown as

$$
\sigma_n^2 = E\{Y^H Y\} - 1
\tag{4.11}
$$

4.4 Expectation Maximization Channel Estimator

Base on the last discussion, we have three methods to obtain the initial channel, and iteration method.

- Initial channel

    4. Pilot Symbol Aided

    5. Linear Prediction

    6. Linear Interpolation

- Iteration- Expectation Maximization

We combine the methods to be six channel estimators

4. EM Algorithm Pilot Symbol Aided　　　(EM Pilot)

5. EM Algorithm Linear Prediction   (EM AR)

6. EM Algorithm Linear Interpolation   (EM LI)

4.5 Channel System Environment

The channel system environments are the same as Chapter 3.5 .

Table 4-1 SUI-3 Channel Model

	Relative delay (μs or sample number)		Average power	
Tap	(μs)	(normal)	(dB)	(normalized)
1	0	0	0	0.7061
2	0.4	4	-5	0.2233
3	0.9	10	-10	0.0706
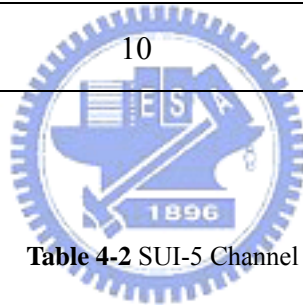
Table 4-2 SUI-5 Channel Model

	Relative delay (μs or sample number)		Average power	
Tap	(μs)	(normal)	(dB)	(normalized)
1	0	0	0	0.7061
2	4	45	-5	0.2233
3	10	112	-10	0.0706

Table 4-3 ETSI "Vehicular A" Channel Model in Different Units

	Relative delay (μs or sample number)		Average power	
Tap	(μs)	(normal)	(dB)	(normalized)
1	0	0	0	0.4850
2	0.31	3	-1	0.3852
3	0.71	8	-9	0.061
4	1.09	12	-10	0.0485
5	1.73	19	-15	0.0153
6	2.51	28	-20	0.0049

4.6 Simulation

We show the simulation result as in Fig. 4-2~Fig. 4-7, there are four cases to be discussing,

■ SUI3 for $v = 100$ km/hr, $v = 240$ km/hr

■ SUI5 for $v = 100$ km/hr, $v = 240$ km/hr

■ Vehicular A for $v = 100$ km/hr, $v = 240$ km/hr

Ts is the sampling time, and F_d is the Doppler frequency, where

$$F_d = vF_c/c$$

■ F_d Doppler frequency

■ F_c carrier frequency

- ■ *v*   velocity of mobile

- ■ *c*   velocity of light

This simulation are base on SUI-3 channel, SUI-5 channel and Vehicular A. The subcarrier number M is 1024, cyclic prefix length $N_{cp} = M/8$. Carrier frequency $F_c = 3.5$ GHz. Bandwidth $BW = 11.2$ MHz, block length $B = 4$ symbols in Linear Interpolation. When Linear Interpolation is used, block length B should not too large, the symbol channels of this block are still linear, so the Linear Interpolation can work. If B is too large, the channels are not linear, so the Linear Interpolation can not work effective.
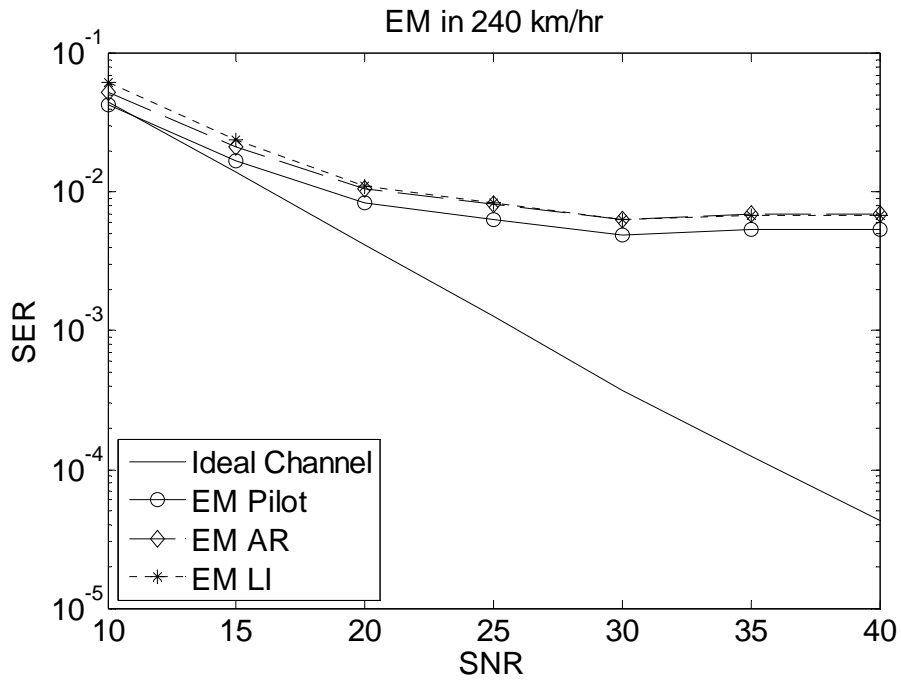
4.6.1 SUI3

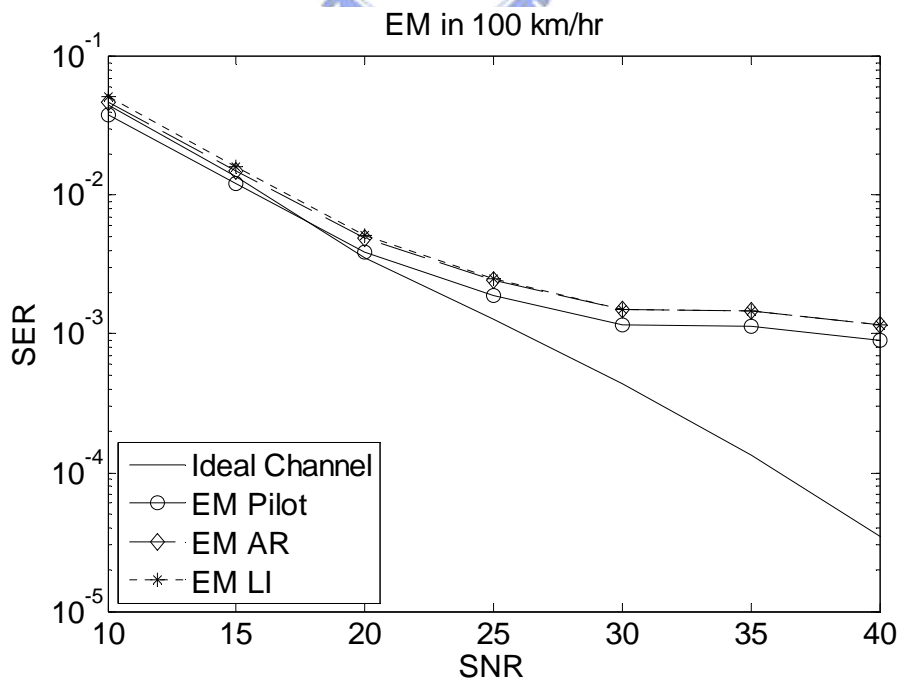**Fig. 4-2** SER performance for EM in 240 km/hr

Fig. 4-3 SER performance for EM in 100 km/hr
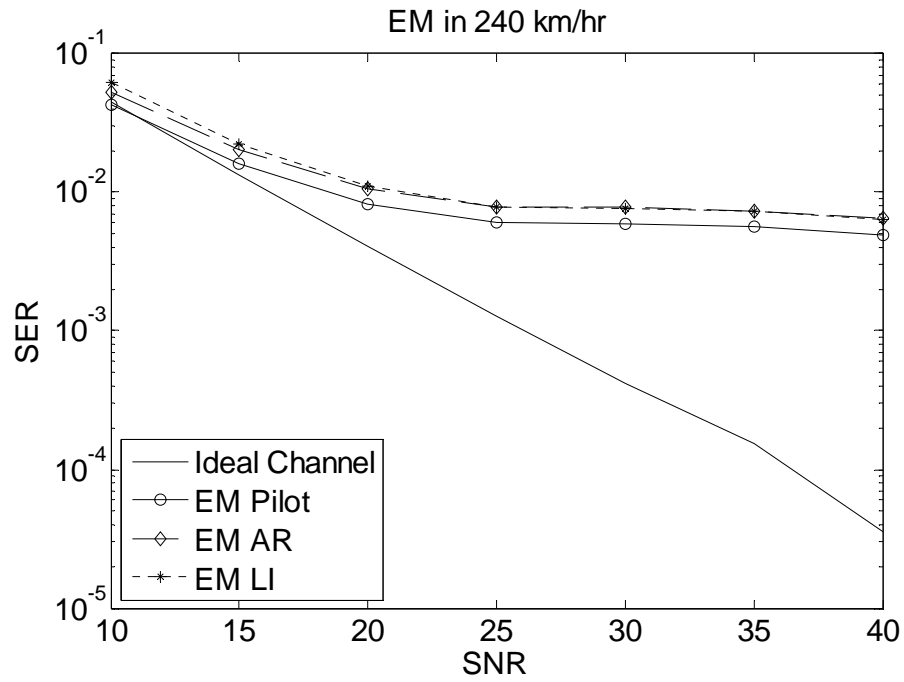
4.6.2 SUI5

Fig. 4-4 SER performance for EM in 240 km/hr
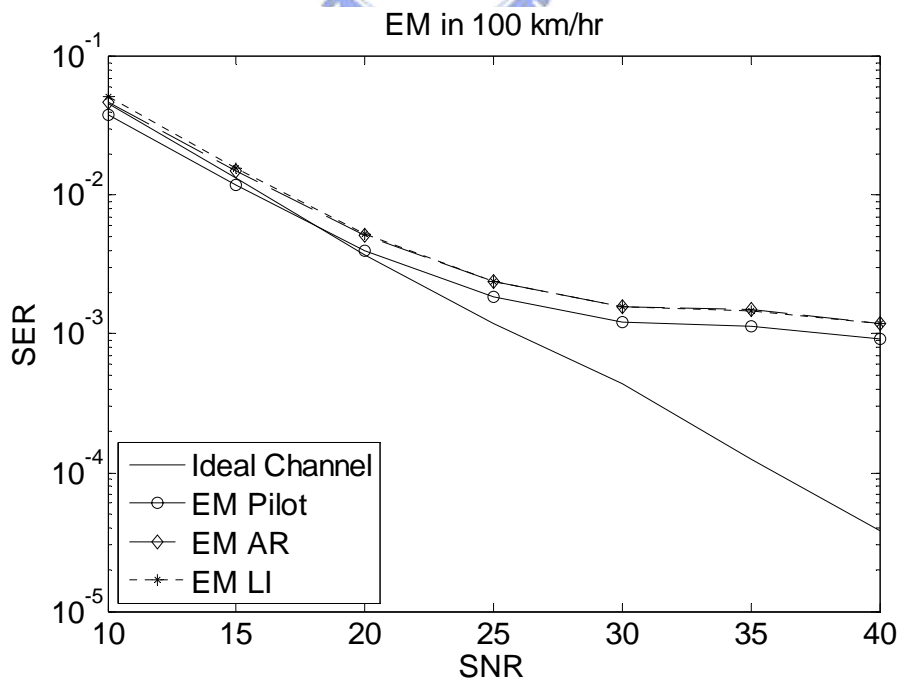

Fig. 4-5 SER performance for EM in 100 km/hr
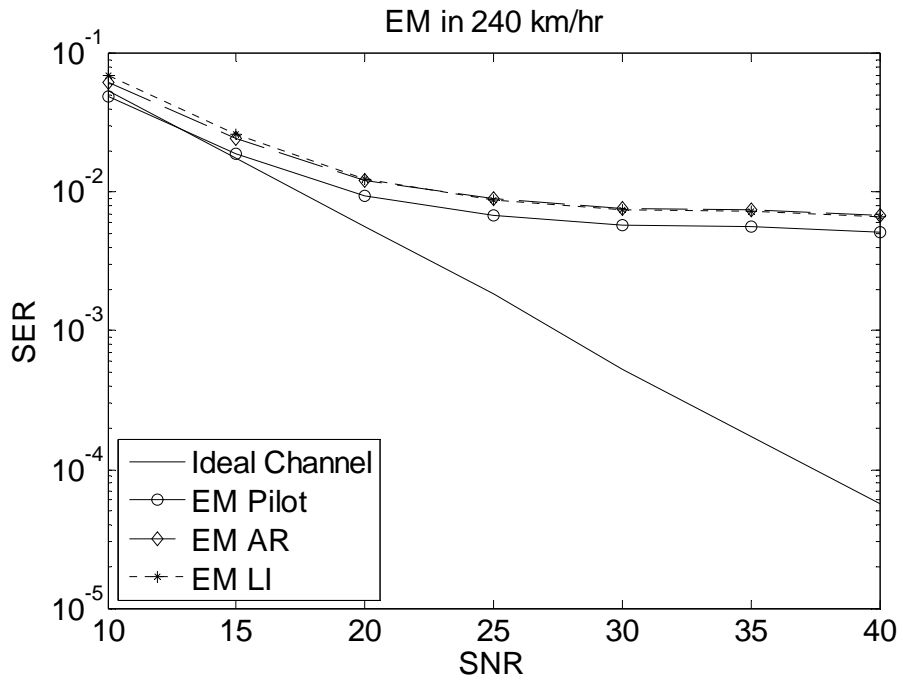
4.6.3 Vehicular A

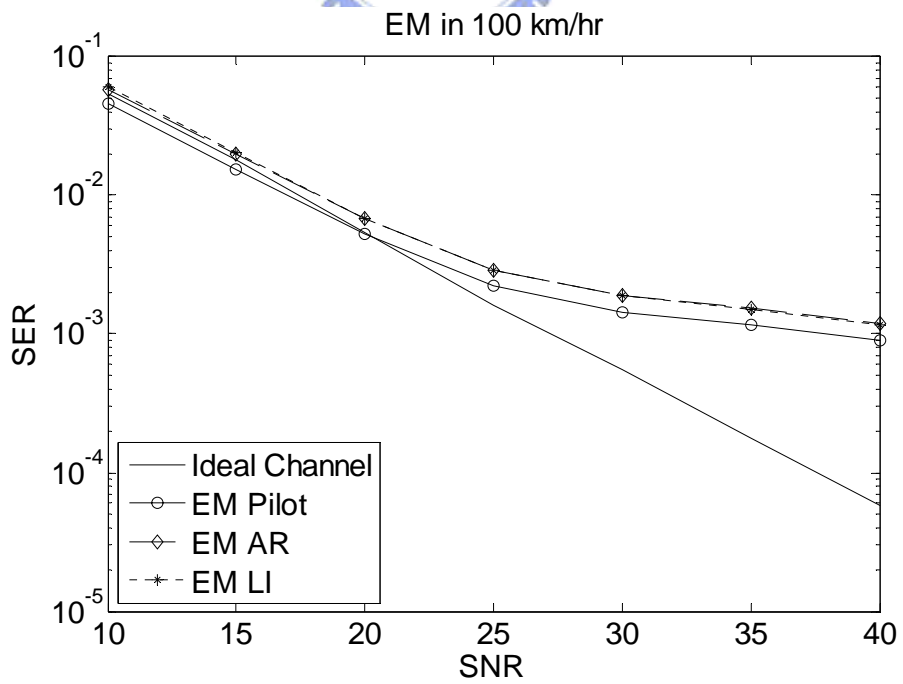**Fig. 4-6** SER performance for EM in 240 km/hr

Fig. 4-7 SER performance for EM in 100 km/hr

According to the simulations, we can see that the performance of the EM-Pilot Symbol Aided has the best SER performance. Just like Decision directed- Pilot Symbol Aided, EM-Pilot Symbol Aided has the highest pilot number. The EM-AR can work very well in each environments, no matter high speed or low speed. The EM-AR method does not use much pilot. When we use Pilot Symbol Aided to obtain the first symbol channel correctly, we can predict next symbol channel without any pilot. The EM-AR can work on time and dose not use any buffer to save data. The EM-Linear Interpolation can work as well as EM-AR, but it has to use some buffer. The buffer is the cost.

Chapter 5
Conclusion

Orthogonal Frequency Division Multiplexing (OFDM) is a popular technique in modern wireless communications. There are many systems adopting the OFDM technique, such as IEEE 802.11 a/g/n, IEEE 802.16, IEEE 802.20, Digital Video Broadcasting, etc. On the other hand mobile transmission is a trend in future wireless communications. For example, IEEE 802.16-2005 supports vehicle speed up to 120 km/hr, IEEE 802.20 supports vehicle speed up to 250 km/hr. Some channel estimator use much pilot to estimate channel, or use buffer to obtain channel. In this thesis, we show one predict-iteration method without pilot and buffer. Finally, we evaluate the performance of the proposed system under mobility using IEEE 802.16-2005 standard and confirm that it achieves good SER performance.

In this thesis, we presented several channel estimation techniques and applied them on Orthogonal Frequency Division Multiplexing (OFDM) system. In Chapter 3, the channel environments and Decision directed Channel Estimation are introduced. We choose SUI-3, SUI-3 and Vehicular A to run the computer simulations. In Chapter 4, the Expectation Maximization Channel Estimation is introduced.

For the result, the EM-AR can work on time and dose not use any buffer to save data. The EM-Linear Interpolation can work as well as EM-AR, but it has to use some buffer. The buffer is the cost. No mater in high speed or low speed, the Expectation Maximization

Channel Estimation can work very well.

References

[1] *IEEE Std 802.16e-2005 and IEEE Std 802.16e-2004/Cor 1-2005*, "Part 16: Air Interface

for Fixed and Mobile Broadband Wireless Access Systems," Feb. 2006.

[2] *IEEE Std 802.16e-2005 and IEEE Std 802.16-2004/Cor1-2005*, IEEE Standard for

Local and Metropolitan Area Networks "Part 16: Air Interface for Fixed Broadband

Wireless Access Systems — Amendment 2: Physical and Medium Access Control

Layers for Combined Fixed and Mobile Operation in Licensed Bands and Corrigendum

1," New York: IEEE, Feb. 28, 2006.

[3] *IEEE Std 802.16e-2004*, "Part 16: Air Interface for Fixed and Mobile Broadband

Wireless Access Systems," Oct. 2004.

[4] *IEEE Std 802.16-2004*, *IEEE Standard for Local and Metropolitan Area Networks* "Part

16: Air Interface for Fixed Broadband Wireless Access Systems," New York: IEEE, June.

2004.

[5] J. A. C. Bingham, "Multicarrier modulation for data transmission: An idea whose time

has come," *IEEE Commun. Mag.*, vol. 28, no. 5, pp. 5-14, May 1990.

[6] R. van Nee and R. Prasad, *OFDM for Wireless Multimedia Communications*. Boston:

Artech House, 2000.

[7] D. Matiae, "OFDM as a possible modulation technique for multimedia application in the

range of mm waves, "http://www.ubicom.tudelft.nl/MMC/Docs/introOFDM.pdf.

[8] J. Puthenkulam, and M. Goldhammer, "802.16 overview and coexistence aspects,"

http://grouper.ieee.org/groups/802/secmail/ppt00009.ppt.

[9]   V.Bykovnikov, "The advantages of SOFDMA for WiMAX,"

http://mail.com.nthu.edu.tw/jmwu/LAB/SOFDMA-for-WiMAX.pdf.

[10] WiMAX Forum, "Mobile WiMAX—Part1:A technical overview and performance

evalution," June 2006,

http://www.wimaxforum.org/news/downloads/Mobile_WiMAX_Part1_Overview_and_

Performance.pdf

[11] H. Yaghoobi, "Scalable OFDMA physical layer in IEEE 802.16 Wireless MAN," *Intel Technology Journal*, vol. 8, pp. 201–212, Aug 2004.

[12] K.-C. Hung and D. W. Lin, "Wireless MAN physical layer specifications: signal processing perspective," Book Chapter, Dec. 2006.

[13] O. Edfors, M. Sandell, J. J. van de Beek, D. Landstrom, and F. Sjoberg, "An introduction to orthogonal frequency-dicision multiplexing," http://courses.ece.uiuc.edu/ece459/spring02/ofdmtutorial.pdf.

[14] J. A. C. Bingham, "Multicarrier modulation for data transmission: an idea whose time has come," *IEEE Commun. Mag.,* vol. 28, no. 5, pp. 5–14, May 1990.

[15] Mauri Nissilä and Subbarayan Pasupathy, "Joint estimation of carrier frequency offset and statistical parameters of the multipath fading channel" *IEEE Transactions on Communications*, vol. 54, no. 6, pp. 1038–1048, June 2006

[16] Xiaoqiang Ma, Hisashi Kobayashi, and Stuart C. Schwartz, "EM-Based Channel Estimation Algorithms for OFDM" *EURASIP Journal on Applied Signal Processing*

2004:10, 1460-1477

[17] Ye(Geoffrey)Li, Leonard J. Cimini, Jr., and NelsonR. Sollenberger, "Robust Channel Estimation for OFDM Systems with Rapid Dispersive Fading Channels" *IEEE Transactions on Communications*, vol. 46, no. 7, pp. 902–915, July 1998

[18] Ye(Geoffrey)Li, "Pilot-symbol-aided channel estimation for OFDM in wireless systems" *IEEE Transactions on Vehicular Technology*, vol. 49, no. 4, pp. 1207–1215, July 2000

[19] V. Erceg et al., "Channel models for fixed wireless applications," *IEEE 802.16.3c-01/29r4, 2004*.

[20] ETSI TR 101 112, "Selection procedures for the choice of radio transmission trchnologeis of the UMTS," *ETSI Technical Report*, V3.0.2, pp. 38-43, Apr. 1994

[21] Ye (Geoffrey) Li, Nambirajan Seshadri, and Sirikiat Ariyavisitakul, "Channel estimation for OFDM systems with transmitter diversity in mobile wireless channels" *IEEE Journal on Selected Areas in Communications*, vol. 17, no. 3, pp. 461–471, March 1999

[22] Michele Morelli and Umberto Mengali, "A comparison of pilot-aided channel estimation methods for OFDM systems" *IEEE Transaction on Signal Processing*, vol. 49, no. 12, pp. 3065–3073, December 2001

[23] Ove Edfors, Magnus Sandell, Jan-Jaap van de Beek, Sarah Kate Wilson, and Per Ola B¨orjesson, "OFDM channel estimation by singular value decomposition" *IEEE Transactions on Communications*, vol. 46, no. 7, pp. 931–939, July 1998

[24] Man-Hung Ng and Sing-Wai Cheung, "Bandwidth-Efficient Pilot-Symbol-Aided Technique for Multipath-Fading Channels" *IEEE Transactions on Vehicular Technology*,

vol. 50, no. 4, pp. 1132–1139, July 2001

[25] Sinem Coleri, Mustafa Ergen, Anuj Puri, and Ahmad Bahai, "Channel Estimation Techniques Based on Pilot Arrangement in OFDM Systems" *IEEE Transactions on Brodcasting*, vol. 48, no. 3, pp. 223–229, September 2002

[26] Xiaodai Dong, Wu-Sheng Lu and Anthony C. K. Soong, "Linear Interpolation in Pilot Symbol Assisted Channel Estimation for OFDM" *IEEE Transactions on Wireless Communications*, vol. 6, no. 5, pp. 1910–1920, May 2007

[27] W. C. Jakes, *Microwave Mobile Communications*. New York: Wiley, 1974.

[28] A. P. Dempster, N. M. Laird, and D. B. Rubin, "Maximum likelihood from incomplete data via the EM algorithm," *Journal of the Royal Statistical Society (B)*, vol. 39, no. 1, pp. 1–38, 1977.

[29] T. K. Moon, "The expectation-maximization algorithm," *IEEE Signal Processing Magazine*, vol. 13, no. 6, pp. 47–60, 1996.

自　　傳

陳錫祺，西元 1979 年生於台北市。 西元 2004 畢業於台灣新竹國立交通大學工業工程與管理學系，之後進入交通大學電子研究所攻讀碩士學位，於 2007 年取得碩士學位。研究方向為無線通訊、通道估測。